

## Glycomacromolecules: addressing challenges in drug delivery and therapeutic development

Will Stuart-Walker and Clare S. Mahon\*

Department of Chemistry, Durham University, South Road, Durham DH1 3LE, UK

Email: [clare.mahon@durham.ac.uk](mailto:clare.mahon@durham.ac.uk)

### Abstract

Carbohydrate-based materials offer exciting opportunities for drug delivery. They present readily available, biocompatible components for the construction of macromolecular systems which can be loaded with cargo, and can enable targeting of a payload to particular cell types through carbohydrate recognition events established in biological systems. These systems can additionally be engineered to respond to environmental stimuli, enabling triggered release of payload, to encompass multiple modes of therapeutic action, or to simultaneously fulfil a secondary function such as enabling imaging of target tissue. Here, we will explore the use of glycomacromolecules to deliver therapeutic benefits to address key health challenges, and suggest future directions for development of next-generation systems.

### Table of Contents

<b>1. Introduction</b> .....	<b>1</b>
<b>2. Glycomacromolecular drug delivery systems to treat cancer</b> .....	<b>2</b>
2.1 Transport and targeting of small molecule drugs .....	3
2.2 Stimuli-responsive glycomacromolecular drug delivery systems .....	5
2.3 Multi-functional delivery systems .....	6
2.4 Delivery of siRNA .....	8
<b>3. Glycomacromolecular drug delivery systems for bacterial infections</b> .....	<b>10</b>
3.1 Targeting drugs to biofilms .....	11
3.2 Glycomacromolecular dispersive agents for biofilms .....	12
<b>4. Glycomacromolecular drug delivery systems for antiviral drugs</b> .....	<b>15</b>
4.1 Human Immunodeficiency Virus (HIV) .....	15
4.2 Influenza .....	16
<b>5. Outlook</b> .....	<b>18</b>

### 1. Introduction

Drug delivery systems have much to offer in improving the treatment of disease. Effective drug delivery systems can selectively target therapeutics to an intended site of action, improving efficacy while minimising harmful side effects. Concurrently, they can protect drugs from environmental conditions and improve the bioavailability of poorly soluble drugs. Delivery systems can additionally provide control over the release profile of a drug, enabling sustained release which can simplify dosing regimes.<sup>1, 2</sup> Drug delivery systems often incorporate macromolecular components such as polymers, liposomes and nanoparticles. These macromolecular architectures possess many useful attributes. In addition to modifying the biodistribution profiles of drugs, their modular nature can enable the construction of systems which simultaneously deliver more than one drug, or combine therapeutic action with a secondary function such as enabling imaging. Through sustained research efforts, it is possible to design highly-targeted delivery systems which respond to external stimuli to enable triggered release of payload.<sup>3-5</sup>

Meanwhile, our understanding of the diverse roles of carbohydrates in biology has advanced significantly. In addition to fulfilling important functions in metabolism, and as structural materials, carbohydrates play crucial roles in enabling cellular recognition. Mammalian cells are decorated with a carbohydrate-rich layer known as the glycocalyx - a complex and diverse mixture of glycoproteins, proteoglycans and glycosaminoglycans - which acts as a cellular 'barcode' for identification.<sup>6</sup> This recognition is key to crucial biological processes which maintain health, yet also underpins many

diverse processes of disease. Many pathogens produce carbohydrate-binding proteins (lectins) which can interact with these complex sugar motifs to facilitate recognition,<sup>7, 8</sup> interactions which often constitute a key step in the processes of infection or disease progression.<sup>9, 10</sup> Characteristic changes in cellular glycosylation patterns, and altered display of cell surface lectins, associated with cancer can provide evidence of disease, and provide a targeting mechanism to direct drugs to these tissues. Consequently, the use of carbohydrates as components within macromolecular drug delivery systems is attractive (Fig. 1). Glycomacromolecular architectures can be accessed via naturally-occurring polysaccharides, or through the attachment of carbohydrates to nanoparticles, or polymeric scaffolds. Alternatively, carbohydrates can be incorporated into lipid bilayers, forming glycovesicles. Polysaccharides can be used to great effect as structural components, offering readily available, biocompatible building blocks for the construction of functional systems. Beyond their use as building blocks, the ubiquity of carbohydrate recognition can be exploited to target drugs to tissues or cell types. Many of these glycomacromolecules display therapeutic properties in their own right, as we will highlight. This factor presents opportunities for the design of multi-functional delivery systems which extend the therapeutic potential of the drug.

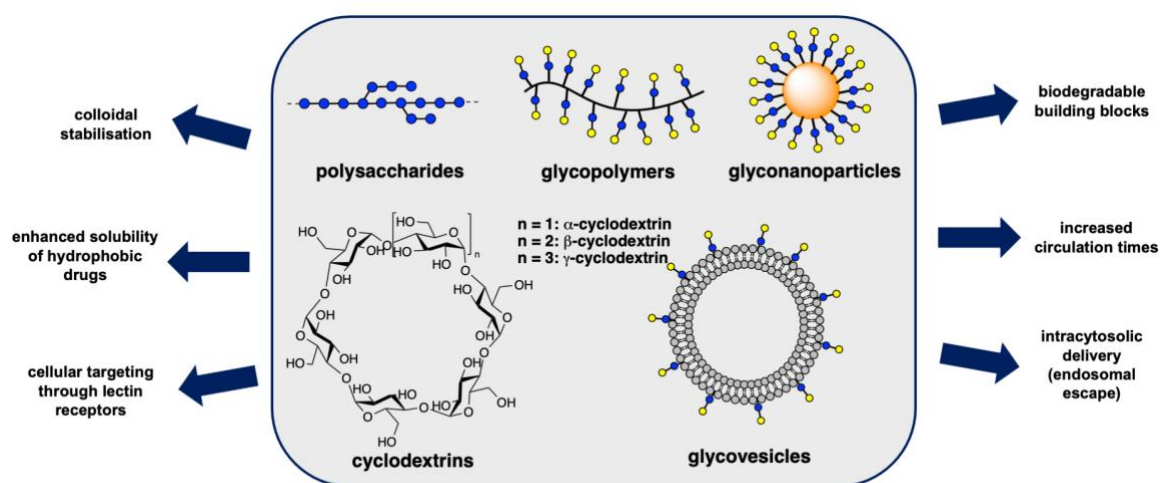


**Fig. 1** Selected glycomacromolecular architectures discussed in this review, and advantages presented by their use in drug delivery systems. Coloured circles represent monosaccharide units.<sup>11</sup>

This review will explore the use of glycomacromolecules to deliver therapeutic benefits to address selected key challenges to human health. We will explore developments in drug delivery to cancer cells, where carbohydrates can act as effective targeting ligands to selectively deliver therapeutics to cancer tissue, presenting a route to the minimisation of side effects. We will next explore the use of glycomacromolecules in tackling bacterial biofilms which contribute to chronic infections and the growing problem of antibiotic resistance, which presents a huge challenge to human health. Finally, we will explore the use of glycomacromolecules in addressing illnesses caused by viruses which account for a major global burden of disease, mindful that the effective treatment of viral pathogens remains a major challenge in contemporary medicinal chemistry.

## 2. Glycomacromolecular drug delivery systems to treat cancer

Cancer is the second most common cause of death globally, estimated to account for 9.6 million deaths in 2018.<sup>12</sup> Many cancer therapies cause debilitating side-effects which could be partially avoided through the selective targeting of therapeutics to cancer cells – *via* a ‘magic bullet.’<sup>13</sup> This challenge is significant, since cancer cells bear many similarities to their healthy counterparts, enabling them to evade the immune system. Excellent advances in immunotherapy and antibody-based targeting systems have been made, with several oncotherapies making it to market. This approach to targeted drug delivery has been well-reviewed elsewhere.<sup>14</sup>

Much research effort is also expended on the design and development of alternative drug delivery systems to enable targeted delivery to cancer cells.<sup>2, 5</sup> In general terms, facilitating the entry of drugs to mammalian cells can be challenging. The permeability of the mammalian cell membrane towards polar or charged molecules through passive diffusion is poor, and the entry of most species, including drugs

and delivery systems, is typically achieved through receptor mediated pathways.<sup>15</sup> Designed drug delivery systems offer many advantages for cancer therapy: they can facilitate the distribution of cytotoxic agents, which are typically poorly soluble, protect the drug from the biological environment until it reaches the desired site of action, and enhance localisation in tumour tissue.<sup>1</sup> Macromolecular systems comprised of polymers, nanoparticles or supramolecular assemblies are particularly well-suited to the delivery of anti-cancer drugs because of their ability to preferentially accumulate in tumour tissue, if their clearance by the reticuloendothelial system can be avoided. This behaviour is known as the enhanced permeation and retention (EPR) effect.<sup>16</sup> Tumour tissue typically displays vasculature with defective architecture, enabling macromolecules to selectively 'leak out' and accumulate in the tissue.

The first macromolecular drug carrier licenced for use was DOXIL®, a PEGylated liposome loaded with doxorubicin which enabled accumulation of the drug in tumours and extended drug circulation times.<sup>17</sup> Liposomes can, however, be recognised as foreign by the reticuloendothelial system, leading to clearance. In early studies, it was noted that incorporation of the mammalian ganglioside GM1 in liposomes significantly extended circulation times through membrane stabilisation effects.<sup>18</sup> Beyond the EPR effect, targeting ligands can enhance the selective delivery of drugs to target tissue, with carbohydrate moieties often proving to be effective. Monosaccharides and oligosaccharides can be recognised by protein receptors that are overexpressed on the surfaces of cancer cells, enabling uptake through receptor-mediated endocytosis. A variety of glycosylated architectures have been explored for this purpose (Fig. 1), including glycopolymers and their assemblies,<sup>19, 20</sup> polysaccharides,<sup>21, 22</sup> vesicles,<sup>23-26</sup> nanoparticles<sup>27-31</sup> and biological scaffolds.<sup>32</sup>

### 2.1 Transport and targeting of small molecule drugs

Cancer cells typically display higher levels of metabolic activity than healthy cells, and often display significantly elevated levels of the glucose receptor GLUT1 on their surfaces.<sup>33, 34</sup> This feature can be exploited to enable the preferential accumulation of glucosylated macromolecular architectures in cancerous cells.<sup>35, 36</sup> Interestingly, GLUT1 has also been shown to recognise dehydroascorbic acid, a feature which has been employed to enable the accumulation of polymer micelles loaded with paclitaxel within tumour cells.<sup>37, 38</sup> Interaction of dehydroascorbic acid with GLUT1 is proposed to proceed via an intramolecular rearrangement to yield a bicyclic hemiketal which bears structural resemblance to D-glucose, highlighting opportunities for the use of glycomimetics<sup>39</sup> as targeting ligands, as an alternative to carbohydrates.

Other carbohydrate ligands also present opportunities for specific targeting. The galectin GAL1,<sup>40</sup> which binds to galactose-terminated glycans, is often overexpressed in tumours,<sup>41</sup> enabling targeting via galactose ligands. Similarly, the asialoglycoprotein receptor (ASGPR)<sup>42</sup> is a C-type lectin that is commonly found on liver cell surfaces which recognises *N*-acetylgalactose- or galactose-terminal glycans. This receptor has been used extensively to selectively target hepatic cells by a range of systems.<sup>31, 32, 43-47</sup> For example, galactosylated block copolymers<sup>20</sup> generated via ring-opening polymerisation self-assembled into micelles, enabling the delivery of doxorubicin to HepG2 cells which display high levels of ASGPR, more effectively than ASGPR negative HEK293 cells.

Some breast cancer cell lines display upregulation of the mannose receptor MRC2<sup>48</sup> which can be exploited to direct the delivery of drugs to cancerous cells. Gupta and coworkers<sup>23</sup> used this recognition to enable targeted delivery of cargo to MDA-MB-231 cells using self-assembled nanocarriers of varied morphologies. A series of miktoarm star polymers containing branched caprolactone chains and glycosylated polypeptide arms were prepared with varying hydrophilic-hydrophobic ratio, resulting in self-assembly of polymerosomes, nanorods or micelles. Polymerosomes and nanorods were successfully taken up by cells via receptor-mediated endocytosis, and demonstrated no cytotoxicity at concentrations of up to 300 µg mL<sup>-1</sup>.

Changes in cellular glycosylation patterns are characteristic of the cancer phenotype.<sup>49</sup> Increased levels of fucosylated glycolipids, for example, have been observed in hepatoma cells.<sup>50</sup> The upregulation of fucose-containing sialyl Lewis<sup>x</sup> and sialyl Lewis<sup>a</sup> antigens has also been noted in many types of cancer.<sup>51</sup> Whilst the cellular uptake mechanism of fucose is not fully understood, cancer cells may be expected to uptake greater quantities of fucose than healthy counterparts, to satisfy the requirements of these altered biosynthetic pathways. With this idea in mind, Stenzel and coworkers<sup>19</sup> prepared amphiphilic block copolymers that were decorated with carbohydrates including fucose, which self-assembled into polymeric micelles. Fucosylated micelles demonstrated higher cell permeability than

glucosylated counterparts in pancreatic cell lines, while simultaneously displaying low levels of internalisation in non-cancerous CHO cells. This approach appears highly promising for the development of drug delivery systems targeting pancreatic cancer, which is traditionally associated with poor clinical outcomes. Fucosylated liposomes have also been used to deliver cisplatin to pancreatic cancer cells.<sup>52</sup> The same delivery system has also been used to deliver SN-38, a DNA topoisomerase inhibitor, to colorectal cancer cell lines.<sup>53</sup> In both cases, the drug-loaded fucosylated liposomes effectively suppressed tumour growth and prolonged survival with no apparent side effects.

Cyclodextrins (Fig. 1) have been used extensively for pharmaceutical applications,<sup>54</sup> and can be used in the construction of targeted drug delivery systems.<sup>55</sup> Ghosh and coworkers<sup>21</sup> have shown that  $\alpha$ -cyclodextrin can interact with tubulin via molecular docking and FRET experiments. In addition to displaying preferential uptake in cancer cells and inhibiting tubulin polymerisation,  $\alpha$ -cyclodextrin could be loaded with curcumin, triggering apoptosis upon delivery. Curcumin-loaded cyclodextrin displayed ~60% cell killing efficiency compared to ~30% for curcumin alone, and was shown to inhibit tumour growth in a HeLa spheroid model. Lactose-modified  $\beta$ -cyclodextrin loaded with doxorubicin<sup>22</sup> was used to deliver the drug to B16 melanoma cells, which display high levels of the GM3 glycolipid. Interestingly, targeting was demonstrated to be a consequence of specific glycan-glycan interactions<sup>56</sup> between lactose and GM3. This delivery system was shown to induce cell death in B16 cells whilst decreasing the proportion of cell death within two other cell lines compared to treatment with doxorubicin alone.

Carbon-based nanomaterials have also been explored as potential drug delivery systems,<sup>57</sup> with some systems employing carbohydrates to solubilise or stabilise the resultant material. Graphene oxide sheets<sup>58</sup> were reduced and covalently modified with chitosan and dextran (Fig. 2) to produce colloidal graphene, which was further decorated with folate to provide a targeting ligand for cellular receptors. The carbohydrate coating stabilised the graphene, preventing aggregation, and the nanocomposite was demonstrated to be non-toxic. The system could be loaded with hydrophobic and hydrophilic drugs or dyes, enabling the simultaneous delivery of multiple cargo species, and enhancing the cytotoxic effects of drugs including doxorubicin and paclitaxel. Carbon nanomaterials can also be employed as templates for the construction of glycosylated drug delivery vehicles. Carbon nanotubes have been used<sup>59</sup> to direct the assembly of diacetylene glycolipids, which were subsequently fixed in place through photopolymerisation. The resultant “glyconanorings” were loaded with camptothecin, and demonstrated enhanced cytotoxicity to MCF7 cells compared to the drug alone.

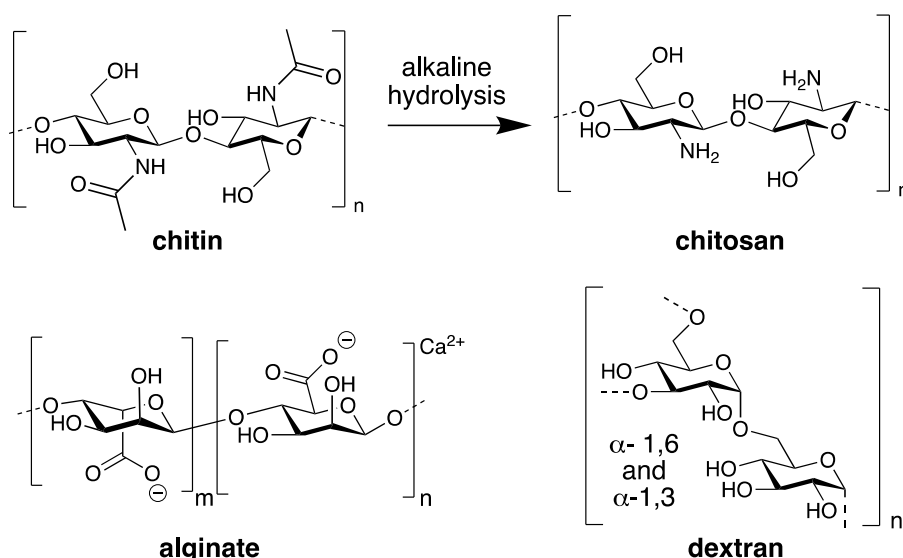


**Fig. 2** Selected polysaccharides used as structural components in the construction of drug delivery systems.

Virus-like particles present an attractive option for the construction of drug delivery systems, offering well-defined, biodegradable nanoarchitectures with excellent cell permeability in some cases.<sup>60</sup> The tobacco mosaic virus (TMV),<sup>61</sup> a plant pathogen which exists as a cylindrical capsid approximately 300 nm in length, was modified<sup>32</sup> with alkyne units and decorated with azido- derivatives of mannose or lactose. Cisplatin was subsequently loaded into the cavity, enabling sustained release of the drug in *in vitro* studies. Mannose-decorated TMV vectors exhibited enhanced endocytosis and cytotoxicity for

MCF7 cells, while lactose-decorated TMV conjugated displayed specific cancer cell targeting ability for HepG2 cells, demonstrating the versatility of glycoconjugates in the development of drug delivery systems.

Effective targeting systems may enable the repurposing of known drugs as anti-cancer chemotherapeutics. The anti-diabetes drug metformin, for example has been demonstrated to display an anti-proliferative effect on numerous cancer cell lines.<sup>62, 63</sup> Long and coworkers<sup>27</sup> have developed a drug delivery system to target metformin to MCF-7 breast cancer cells. Gold nanoparticles (AuNPs) were decorated with dextran, which was subsequently oxidised to enable the attachment of metformin via dynamic imine linkages. Dextran-coated AuNPs demonstrated improved cell permeability and enhanced the anti-proliferative effect of metformin on MCF-7 cells, whilst healthy cells treated with the conjugate displayed good cell viability.

## 2.2 Stimuli-responsive glycomacromolecular drug delivery systems

The advent of “smart” materials<sup>64, 65</sup> has enabled the design of drug delivery systems capable of releasing their cargo in response to an environmental trigger,<sup>5</sup> ideally after localisation at the desired site of action. Environmental stimuli that can be employed to induce release of cargo include changes in pH, with the tumour microenvironment typically displaying pH in the range 5.5-7.0,<sup>66</sup> lower than that observed in healthy tissue, and reduction potential, with cytosolic glutathione (GSH) concentrations in the millimolar range, compared to micromolar concentrations in plasma.<sup>67</sup> These strategies can enable more precise delivery of drugs to cancer cells, and show great promise for the development of next-generation cancer therapies with improved side effect profiles.

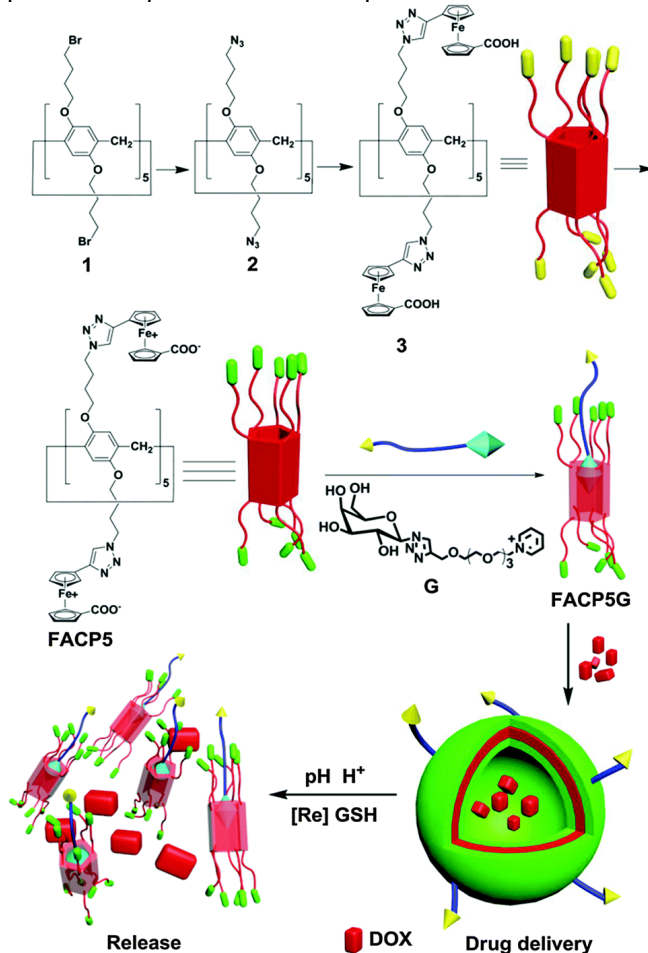


**Fig. 3** Redox-responsive vesicles enable the delivery of doxorubicin to tumour cells, with release triggered by application of pH and redox stimuli. Reproduced from ref. 25 with permission from The Royal Society of Chemistry.

In one such example,<sup>25</sup> a ferrocene carboxylic acid-capped pillar[5]arene was used to construct a host-guest complex with a pyridinium-modified galactose derivative which subsequently self-assembled in the presence of doxorubicin to form redox-responsive vesicles (Fig. 3). Vesicles were shown to disassemble only upon addition of GSH in an acidic environment (pH 4). Doxorubicin release was rapid under model tumour conditions of reduced pH and high GSH concentration. Treatment of MCF7 cells displaying a complementary galectin yielded lower cell viabilities than treatment with free doxorubicin. In contrast, non-cancerous cells displayed higher viabilities when treated with doxorubicin-loaded vesicles compared to free doxorubicin. Liu and coworkers<sup>31</sup> prepared AuNPs stabilised with thiol-modified galactose residues and further modified via boronic acid formation with a disulfide-linked prodrug or imaging agent (Fig. 4). The nanoparticles were internalised by HepG2 cells, where high intracellular glutathione concentrations triggered an intramolecular cyclisation to release the payload, leading to cytotoxicity. The system displayed good biocompatibility for cell lines which do not display the ASGPR.

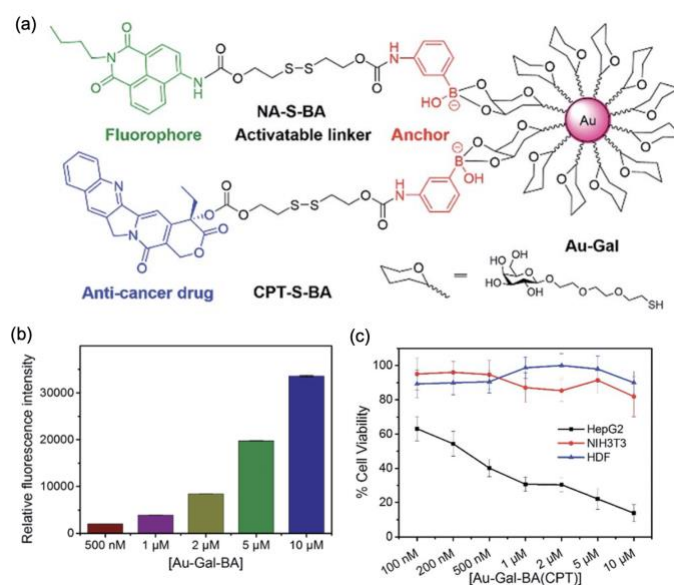


**Fig. 4** (a) A redox-responsive multivalent glyconanoparticle platform for drug delivery and imaging, prepared by Liu and coworkers.<sup>31</sup> (b) Internalisation of glyconanoparticles in HepG2 cells, as determined by flow cytometry. (c) Cell viabilities of ASGPR-displaying HepG2 cells, and control cell lines, upon treatment with glyconanoparticles as measured using WST-1 assays. Reproduced with permission from reference 31, published by the Royal Society of Chemistry.

Jayakannan and coworkers<sup>24</sup> constructed vesicles using partially oxidised dextran modified with hydrophobic sidechains via ester linkages. Doxorubicin could be loaded within the vesicles or conjugated onto the dextran scaffold via imine linkages. The vesicles were responsive both to decreases in environmental pH and the presence of esterases. Complete release of payload could be triggered by the simultaneous application of both stimuli in *in vitro* conditions simulating the intracellular environment, whilst cell studies demonstrated penetration and improved cytotoxicity in MCF7 cells. A glucose modified peptide<sup>36</sup> displaying a matrix metalloproteinase (MMP) sensitive sequence was used to transport PAMAM dendrimers into MCF7 cells through interaction with the GLUT1 receptor. Within the cell, the glucose targeting ligand was removed via the action of MMP, and a triphenylphosphine targeting ligand enabled intracellular trafficking of the dendrimers to mitochondria. Redox-triggered release of paclitaxel led to cytotoxicity, with improved suppression of tumour growth compared to free paclitaxel in a mouse model.

### 2.3 Multi-functional delivery systems

The use of macromolecular species or assemblies in drug delivery presents the opportunity to design systems with multiple modes of action. The term 'theranostics'<sup>68</sup> refers to materials that combine a diagnostic signal with a therapeutic effect. Systems that could enable imaging of tumour tissue combined with localised delivery of anticancer drugs are particularly attractive, and many excellent

examples exploit carbohydrate targeting ligands to direct the theranostic to the site of action. Photodynamic therapy (PDT)<sup>69</sup> is a non-invasive alternative to chemotherapy or radiotherapy which can currently be used effectively to treat some epithelial cancers. PDT involves the use of photosensitisers which, upon irradiation, generate reactive oxygen species such as singlet oxygen ( $^1O_2$ ), which destroys surrounding tissue. Improvements in delivery of photosensitisers to tumours, combined with two-photon approaches to activation<sup>70</sup> which enable the use of lower energy light, which penetrates tissue to a greater extent, would expand the range of cancers PDT could be used to treat.

In one such example, a lactose moiety was appended<sup>43</sup> to a dicyanomethylene-4*H*-pyran (DCM) unit via a redox-responsive linker. The resulting amphiphile self-assembled to form spherical vesicles which could be loaded with doxorubicin to enable its selective delivery to HepG2 cells displaying the complementary ASGPR. Reduction induced cleavage of the amphiphile by intracellular GSH led to activation of the NIR-probe and facilitated delivery of doxorubicin. Demonstrating the versatility of glyco-targeted PDT systems, He and coworkers<sup>45</sup> incorporated galactose or mannose DCM derivatives into core-shell nanodots generated by the self-assembly of poly(3-hexylthiophene-2,4-diyl), a polymer commonly used in the fabrication of optoelectronic devices, and poly(styrene-co-maleic anhydride). The carbohydrate ligands enabled effective delivery to cells displaying a complementary cell surface receptor, with galactosylated nanodots shown to localise in HepG2 cells, while mannosylated nanodots displayed preferential uptake in MDA-MB-231 cells. Irradiation resulted in the death of targeted cell lines, while the nanodots were shown to be non-toxic to healthy cell lines, irrespective of irradiation. In a strategy<sup>44</sup> combining receptor-targeted cell imaging, PDT and conventional anticancer chemotherapeutics, AuNPs functionalised with cyclodextrin were used to form nanocomposites with a galactose-modified naphthalimide through cyclodextrin-adamantane interactions (Fig. 5). Naphthalimide fluorescence was initially quenched through FRET to the proximal AuNPs, but was restored upon exposure to a galactose-binding lectin, or HepG2 cells displaying a transmembrane galactose receptor, enabling targeted imaging. The nanocomposites were loaded with the anti-cancer drug hydroxycamptothecin, and were shown to significantly enhance its cytotoxicity. Irradiation with light at 600 nm further enhanced the cytotoxicity of the nanocomposites through the production of reactive oxygen species, displaying dual therapeutic potential.

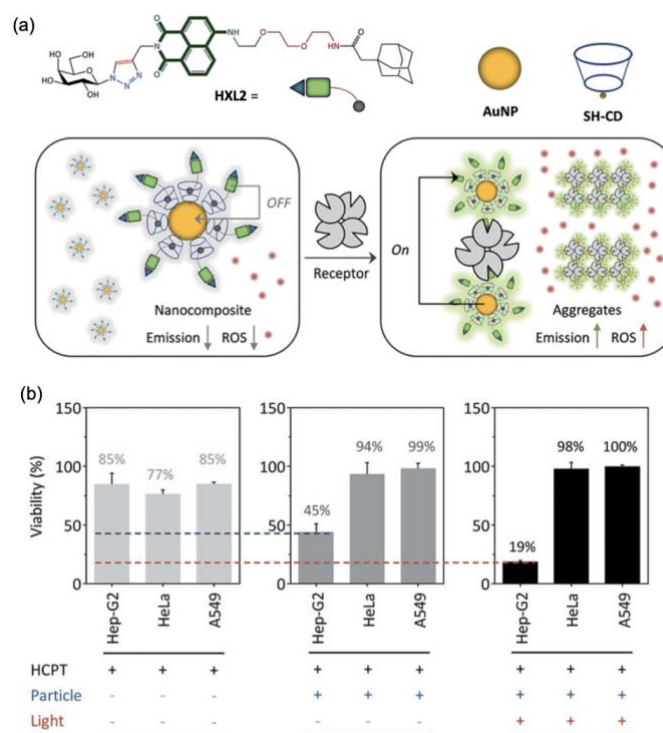


**Fig. 5** (a) Galactose-displaying nanocomposites produced by Hu *et al.*<sup>44</sup> Upon exposure to galactose binding lectins or cells bearing the ASGPR, aggregation leads to enhancements in fluorescence emission and production of ROS. (b) Cell viabilities of ASGPR-displaying HepG2 cells, and control cells, upon treatment with hydroxycamptothecin (HCPT), HCPT loaded within nanocomposites, and HCPT

loaded nanocomposites with irradiation at 600 nm. Reproduced with permission from reference 44, published by the Royal Society of Chemistry.

Theranostic systems are particularly attractive for cancers which are difficult to treat, where early detection can significantly improve patient outcomes. Triple-negative breast cancers<sup>71</sup> are one such example, with difficulties in providing targeted treatment arising as cells lack overexpression of three key cell surface receptors which can otherwise be used to direct uptake of anticancer drugs: the oestrogen and progesterone receptors, and the human epidermal growth factor 2. Some triple negative breast cancer cell lines have been noted to overexpress the mannose receptor CD206, enabling the delivery of mannose glycoconjugates via receptor-mediated endocytosis.<sup>55, 72</sup> In one approach,<sup>73</sup> mannose-functionalised BODIPY dyes were incorporated into micelles, enabling selective uptake and imaging of triple-negative MDA-MB-231 cells. The cytotoxicity of the micelles was shown to be negligible in the absence of light, but irradiation led to the generation of <sup>1</sup>O<sub>2</sub> and subsequent apoptosis. In another recent example,<sup>74</sup> two dimensional “glycoclusters” were generated through the assembly of MnO<sub>2</sub> nanosheets with human serum albumins complexed with a mannose-functionalised DCM derivative, and chlorin e6, a tetrapyrrole-derived photosensitiser. Glycoclusters were selectively taken up by MDA-MB-231 cells, enabling imaging by fluorescence microscopy. Upon irradiation with light at 660 nm, significant decreases in cell viability were observed, whilst the viability of HeLa cells which do not overexpress CD206 remained high. In a mouse xenograft model, the glycoclusters were shown to preferentially accumulate in tumour tissue, demonstrating promise as a theranostic system *in vivo*.

#### 2.4 Delivery of siRNA

Short interfering RNA (siRNA) therapy can disrupt the biosynthesis of essential proteins by ‘silencing’ the expression of a gene with a complementary sequence, interfering with cellular pathways and presenting an attractive route to the treatments of many cancers. The *in vivo* efficacy of siRNA is restricted because of its instability to RNase enzymes in the bloodstream and its multiple negative charges, leading to rapid degradation.<sup>75</sup> Achieving intracellular uptake, and subsequent intracytosolic release of siRNA poses a major challenge to its therapeutic use. Delivery systems incorporating polymers or liposomes which complex siRNA can enable significant improvements in function.<sup>76</sup>

siRNA delivery systems commonly rely on interpolyelectrolyte complexation to form stable nanosized assemblies, commonly termed polyplexes. Many conventionally-used cationic synthetic polymers such as polyethyleneimine (PEI) display cytotoxic effects, however.<sup>77</sup> Polysaccharides can present alternative, biocompatible building blocks for the construction of delivery systems, and can display similar ‘stealth’ properties to PEGs.<sup>78</sup> Poly(D-glycoamidoamines) have been extensively investigated by Reineke and coworkers,<sup>79-85</sup> enabling the formation of polyplexes with siRNA which are readily internalised by a range of cell types and can facilitate effective gene silencing. The first system to enable targeted delivery of siRNA in humans was developed by Davis and coworkers,<sup>86</sup> based on a system that has been used previously to deliver plasmid DNA.<sup>87</sup> Cyclodextrin-containing cationic polymers were complexed with siRNA to form polyplexes, with adamantane-modified PEG chains providing steric stabilisation.<sup>88-91</sup> Incorporation of a transferrin-targeting ligand enabled targeted delivery to tumour tissue.<sup>92, 93</sup> A Phase I clinical trial demonstrated that the polyplexes localised in tumour tissue and achieved specific gene inhibition, reducing the expression of the targeted protein, RRM2, an enzyme involved in DNA synthesis.<sup>94</sup>

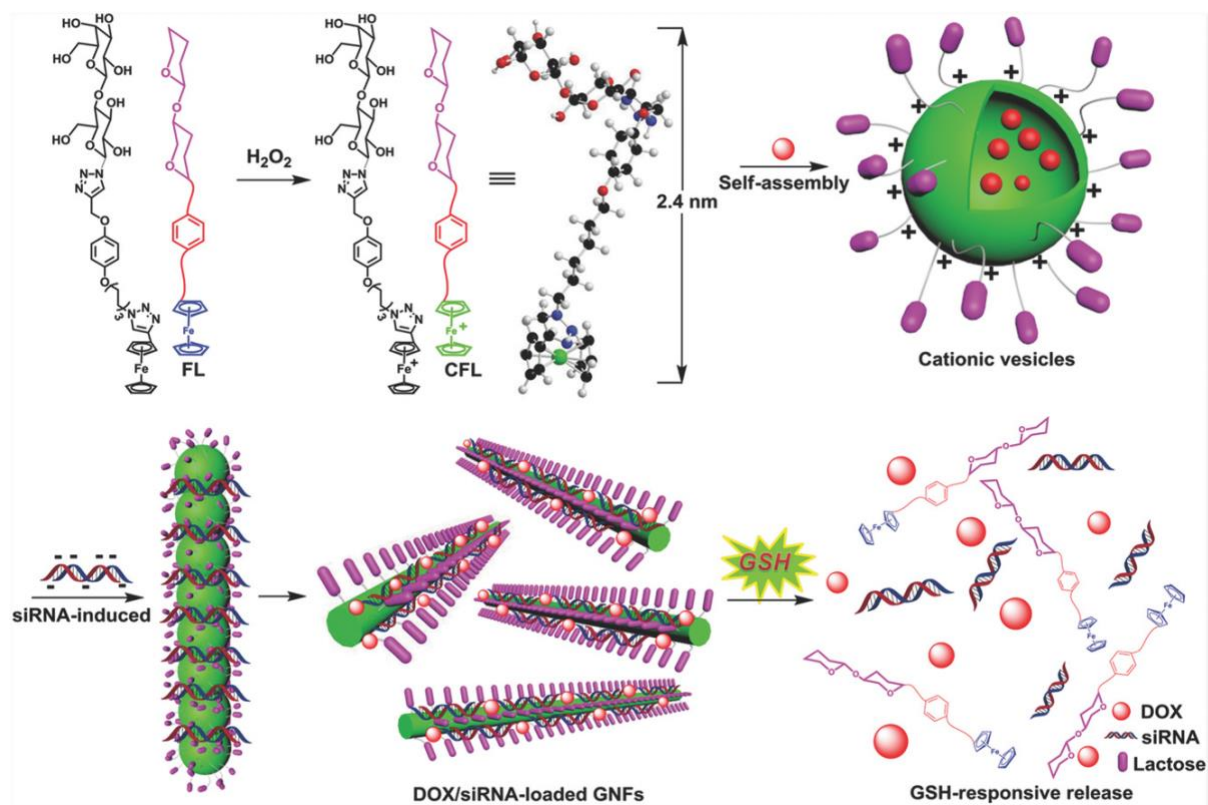


**Fig. 6** A dual-action drug delivery system constructed by the complexation of lactose-modified redox-responsive vesicles with siRNA. Glyconanofibres could be loaded with doxorubicin, with exposure to GSH inducing disassembly and release of both cargo. Reprinted with permission from *Adv. Funct. Mater.*, 2017, **27**, 1703083, Copyright 2017 John Wiley and Sons.

Stimuli-responsive systems have also been designed to enable triggered release of siRNA. In one such example,<sup>95</sup> a thiol-modified chitosan derivative was used to form complexes with poly(siRNA)s containing disulfide linkages, with intramolecular crosslinking leading to stable nanoarchitectures. This system enabled rapid cellular internalisation and effective gene silencing. Targeting the vascular epithelial growth factor (VEGF) gene lead to 80% reduction in tumour size in a mouse model. Combining siRNA-based gene silencing with conventional chemotherapy, Pei and coworkers<sup>46</sup> prepared doxorubicin-loaded cationic glycovesicles through the self-assembly of a lactose-displaying amphiphile containing a redox-responsive ferrocenium unit (Fig. 6). Addition of siRNA led to interpolyelectrolyte complexation to yield glyconanofibres which could enter HepG2 cells and disassemble in response to high intracellular GSH concentration, releasing the cargo. Glyconanofibres displayed high transport efficiency, effective gene silencing and enhanced cytotoxicity in *in vitro* experiments, combined with effective tumour targeting in a mouse model.

Synthetic glycopolymers offer an attractive approach to the development of delivery systems for siRNA, enabling precision design of the components of the system. Cationic glycopolymers have been used effectively in the delivery of plasmid DNA to mammalian cells.<sup>96-98</sup> Advances in controlled/‘pseudo-living’ polymerisation methods<sup>99-102</sup> allow for the synthesis of highly tailored polymers, enabling the effects of structural features such as monomer composition and distribution (block- vs statistical copolymers) and particle size to be probed. Narain and coworkers<sup>103</sup> prepared a selection of block and statistical copolymers of 2-aminoethylacrylamide (AEMA) and 2-lactobionamidoethyl methacrylamide which were subsequently complexed with siRNA. The resultant polyplexes demonstrated comparable gene silencing of the tumour-associated epidermal growth factor receptor (EGFR) gene to a conventional PEI-based system. The effects of monomer distribution on cytotoxicity were explored, with polyplexes constructed using diblock copolymers displaying higher levels of cellular toxicity than the analogous statistical copolymers. In a subsequent study,<sup>104</sup> hyperbranched polymers constructed using these monomer units, combined with an acid-sensitive crosslinker, were demonstrated to enable enhanced silencing of the EGFR gene whilst maintaining ~80-100% levels of cell viability 48 h after transfection. In related work by the same group,<sup>105</sup> poly(glycidyl methacrylate) scaffolds were decorated with ethanolamine and a lactobionic acid derived aminosaccharide in differing ratios. The effects of

monomer composition on cytotoxicity and transfection efficiency were investigated in HeLa cells. Polymers with a higher degree of lactobiose incorporation displayed the highest levels of biocompatibility, but less effective gene silencing, an effect proposed to arise from the lower surface charge of these species, which may impede intracellular delivery.

Most siRNA delivery systems employ electrostatic interactions to enable complexation with siRNA. In an elegant alternative strategy,<sup>47</sup> polymer scaffolds were modified with *N*-acetylgalactose units to facilitate cellular targeting, and melamine moieties to enable complexation with nucleobases. Glycopolymers were demonstrated to form complexes with native and synthetically modified siRNAs, and to deliver siRNA to HepG2 cells bearing the complementary ASGPR. This system displayed low cytotoxicity and enabled highly effective silencing of the ApoB gene, with IC<sub>50</sub> values in the low nanomolar range reported.

In addition to facilitating cellular targeting, carbohydrates can also confer physical stabilisation on siRNA delivery systems.  $\alpha,\alpha$ -D-trehalose, a disaccharide of glucose, and corresponding glycoconjugates have been observed to stabilise biomacromolecules to environmental stresses such as changes in temperature.<sup>106</sup> Reineke and coworkers<sup>107</sup> prepared diblock copolymers of AEMA and a methacrylamido-trehalose derivative via RAFT polymerisation, and complexed the polymers with siRNA. Polyplexes exhibiting multivalent display of trehalose allowed for effective delivery of siRNA and gene silencing in glioblastoma cells which overexpressed the GLUT1 receptor. Polyplexes could also be lyophilised and reconstituted without loss of function, addressing a key practical challenge in the realisation of siRNA therapeutics.

### 3. Glycomacromolecular drug delivery systems for bacterial infections

Bacterial infections present a major burden of mortality and morbidity, with the growing problem of antimicrobial resistance predicted to cause major challenges for healthcare systems and economies on a global scale.<sup>108</sup> The development of effective drug delivery systems to combat bacterial infections is complicated by the diverse range of phenotypes presented by pathogenic bacteria. Infections may be intracellular, or extracellular, either in a planktonic ('free-floating') state or an adherent mode. Bacterial cells additionally present a diverse range of surface topologies and chemical features, with properties such as surface charge that vary between species and growth stages.<sup>109</sup>

The importance of carbohydrate recognition in the progression of bacterial infections is increasingly recognised. Often glycan motifs displayed on the cellular surface are exploited by bacterial lectins to enable adhesion, or the entry of toxins.<sup>9</sup> Multivalent glycoconjugates based on macromolecular scaffolds<sup>9, 39</sup> have been explored as potential antiadhesive therapies,<sup>110</sup> presenting the opportunity to develop new treatments that do not rely on antibiotic effects. Simple carbohydrate motifs can prove successful in binding to bacterial proteins, exploiting the cluster glycoside effect to enable high avidity recognition.<sup>111</sup> Multivalent display of glucose on polymer nanoparticles, for example, has been demonstrated to induce the aggregation of *E. coli* and *S. aureus*, and nanoparticles could be loaded with ampicillin to exert a bactericidal effect.<sup>112</sup> Mannosylated nanogels containing phosphodiester linkages have been used to deliver drugs such as vancomycin to the sites of MRSA infection in a zebrafish model.<sup>113</sup> These nanogels can bind to mannose receptors on the surfaces of macrophages, enabling their transport to the site of an infected wound, where bacterial phosphatases then act to release the antibiotic. In another stimuli-responsive system, boronic acid functionalised halloysite nanotubes<sup>114</sup> were loaded with pentoxifylline and incorporated into a starch hydrogel. Treatment of hydrogels with H<sub>2</sub>O<sub>2</sub> to simulate oxidative stress led to release of the drug, demonstrating potential for use in wound dressings.

The treatment of intracellular bacterial infections poses another set of challenges. Gluconamide, an acyclic carbohydrate bearing structural resemblance to regions within the Gram-negative lipopolysaccharide matrix, has been grafted onto the surface of SiO<sub>2</sub> nanoparticles (SiO<sub>2</sub>-NPs).<sup>115</sup> The carbohydrate coating avoided the formation of a protein corona around the SiO<sub>2</sub>-NPs and prevented their aggregation in serum. When glycosylated SiO<sub>2</sub>-NPs were loaded with tetracycline, a 5-fold decrease in MIC was observed. Glycosylated SiO<sub>2</sub>-NPs displayed no haemolytic activity in mammalian cell viability assessments, in contrast to uncoated SiO<sub>2</sub>-NPs, and were internalised by cells, presenting opportunities for to target intracellular bacterial infections.

### 3.1 Targeting drugs to biofilms

In many cases, initial colonisation by pathogenic bacteria can lead to the formation of biofilms: complex, often polymicrobial communities of bacteria typically associated with persistent infections. Biofilms are implicated in a diverse range of conditions,<sup>116</sup> including chronic infections of wounds and around medical implants,<sup>117</sup> and in persistent respiratory infections in patients with cystic fibrosis (CF).<sup>118</sup>

Within a biofilm, bacteria are bound within a matrix of extracellular polymeric substances (EPS), which accounts for most of the mass of the biofilm.<sup>116</sup> The EPS is comprised of secreted polysaccharides, proteins, lipids and extracellular DNA, which assemble into a crosslinked matrix which fulfils diverse functions for the microorganisms within, enabling resource capture, regulation of the physicochemical environment, and presenting a physical barrier to the delivery of antibiotics, often frustrating the treatment of these infections and contributing to the progression of antibiotic resistance.

The architecture of the biofilm arises primarily through supramolecular interactions between components of the EPS, including hydrogen bonds and electrostatic interactions, such as those found between cationic polysaccharides and extracellular DNA.<sup>119</sup> Disruption of the EPS matrix to enable effective delivery of drugs to bacteria within biofilms is an active area of research.<sup>120</sup> More effective delivery of drugs to bacteria could enable improvements in the performance of existing drugs, reducing the need for the development of novel bactericidals. Precisely-targeted delivery to pathogenic bacteria could also potentially limit the extent to which other bacteria within a microbial community are exposed to the sub-lethal concentrations of antibiotics associated with the development of resistance. Owing to the polyanionic nature of extracellular DNA, a key component of the EPS, positively-charged polysaccharides such as chitosan have attracted interest for the disruption of biofilm architecture.<sup>121-123</sup> Chitosan is readily available through the deacetylation of chitin (Fig. 2) obtained from the shells of crustaceans, and has been demonstrated to itself display antimicrobial properties, though modest.<sup>124</sup>

Chitosan is a useful building block in drug delivery systems.<sup>125-129</sup> Birk and coworkers<sup>125</sup> spray-coated chitosan to cap polymer microcontainers loaded with ciprofloxacin (Fig. 7). After an initial burst, sustained release of the drug was observed over a 28 h period in an in vitro study, compared to ~7 h for 'open' or PEG- capped ciprofloxacin-loaded microcontainers. This release profile was proposed to be consistent with slow but constant diffusion of ciprofloxacin through a chitosan hydrogel. Chitosan-capped microcontainers loaded with ciprofloxacin demonstrated an impressive bactericidal effect in *P. aeruginosa* biofilms, with  $88.2 \pm 5.3\%$  of the biomass of preformed PAO1 biofilms attributed to dead cells after 24 h of treatment with microcontainers.

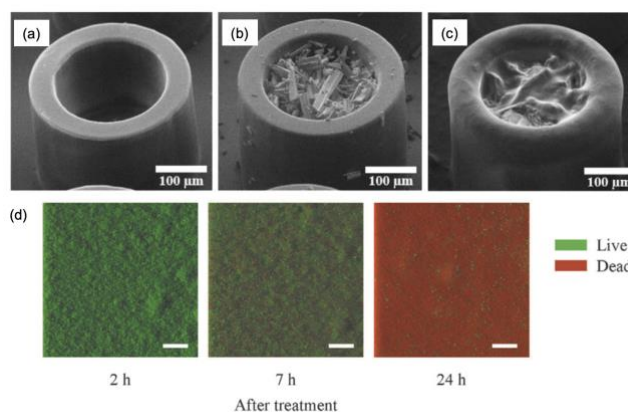


**Fig. 7** Microfabricated containers, (a) loaded with ciprofloxacin, (b) and capped with chitosan, (c), enable sustained release of the drug to *P. aeruginosa* biofilms, (d) significantly reducing the live population within the biofilms.<sup>125</sup> Reproduced (adapted) from reference 125 with permission.

One advantage of using composite systems is the opportunity to employ multiple strategies to disrupt the biofilm. Tan and coworkers<sup>126</sup> used chitosan nanoparticles to simultaneously deliver an antibiotic, oxacillin, and DNase to disrupt the EPS structural integrity. This system was demonstrated to inhibit biofilm formation of *S. aureus* at concentrations lower than those required for treatment with antibiotic

alone, and effectively disrupt pre-formed biofilms, including in strains of clinical origin. A similar approach has recently been used to deliver alginate lyase,<sup>128</sup> and enzyme targeting secreted polysaccharide, and ciprofloxacin to *P. aeruginosa* biofilms, reducing live cell density and biomass.

In many species, the formation of biofilms may be regulated by nitric oxide (NO).<sup>130</sup> NO-based therapies have proven useful in some cases, e.g. through topical application or inhalation, but applications are limited in scope because of difficulties in administering a gaseous drug, in addition to the instability of NO in biological media.<sup>131</sup> The development of NO delivery vehicles is an active area of research,<sup>132</sup> and small-molecule NO donors have been incorporated onto macromolecular scaffolds such as polymers<sup>133-135</sup> and dendrimers<sup>136</sup> to enable its effective delivery to biofilms. Chitosans with molecular weights between 2.5-10 kDa, prepared via an oxidative degradation strategy, were modified to install *N*-diazoniumdiolate units, enabling the storage and release of NO.<sup>137</sup> These oligosaccharides were demonstrated to eradicate *P. aeruginosa* biofilms without displaying toxicity in cell viability experiments. NO-releasing chitosan oligosaccharides were later shown to decrease the viscoelasticity of CF sputum,<sup>138</sup> demonstrating a mucolytic action similar to commonly used therapeutics, suggesting that these systems could function as dual-action treatments for CF-related lung infections.

Naturally-sourced chitin displays heterogeneity in structure, both in terms of its degree of polymerisation and the extent of deacetylation. Often, the precise composition of the material under study is often poorly defined or unknown, potentially presenting problems with reproducibility if chitosan-based systems were to be employed on a large scale. The degree of acetylation, for example, which varies according to the conditions used in the preparation of chitosan from chitin, will affect intermolecular self-assembly processes. The effects of varying structural parameters of chitin have been largely underexplored, however, in favour of investigating the effects of chemical modifications to a pre-formed chitosan scaffold.<sup>139</sup> One study<sup>140</sup> has investigated the effects of molecular weight on efficacy using two chitosan oligosaccharides of varied degree of polymerisation ( $M_w$  835 g mol<sup>-1</sup>, 1419 g mol<sup>-1</sup>), produced via a controlled degradation process. Streptomycin was attached to chitosan oligosaccharides via an imine linkage, and the conjugate was used to deliver streptomycin to *P. aeruginosa* biofilms. After 24 h, the mass of biofilm was found to be reduced by >70% in both cases. Interestingly, treatment with streptomycin-chitosan conjugates was observed to lead to downregulation of genes associated with the MexXY multi-drug efflux system, which is usually activated when *P. aeruginosa* is treated with streptomycin.<sup>141</sup> Additionally, downregulation in the expression of genes associated with exopolysaccharide production (*pelA*, *algD*) was observed, suggesting that the conjugates may damage the structural integrity of the biofilm, in addition to exerting a bactericidal effect. In this study, the conjugate constructed using the higher molecular weight oligosaccharide was shown to be more effective, suggesting that structural features of chitosan could be explored in order to optimise the efficacy of drug-delivery systems. Improvements in methods for the controlled preparation of oligo/polysaccharide materials through enzymatic<sup>142</sup> or solid-phase<sup>143</sup> approaches presents the opportunity to define structure-function relationships for these and other polysaccharide-based systems.

### 3.2 Glycomacromolecular dispersive agents for biofilms

In addition to enabling the targeted delivery of therapeutics to biofilms, polysaccharide species used in the construction of drug delivery systems can also display therapeutic benefits of when used alone, presenting exciting opportunities for the development of multi-action systems. Alginates are linear copolymers of  $\beta$ -(1,4)-linked D-mannuronic and L-guluronic acid that can be obtained from natural sources such as seaweed.<sup>144</sup> Alginates are non-toxic and display good biocompatibility,<sup>145</sup> presenting an attractive option for biomedical use. In *P. aeruginosa*, alginates form an important structural component of mucoid biofilms.<sup>144</sup> Low molecular weight analogues have demonstrated impressive potential in the dispersal of biofilms of *P. aeruginosa* and other species.<sup>146-149</sup> A 12-15mer alginate derived from plant biopolymers, OligoG, has been shown to reduce proliferation of a number of bacterial species including *P. aeruginosa*, *Acinetobacter baumannii*, *Burkholderia* spp. and *Enterobacteriaceae*.<sup>146</sup> Preliminary studies demonstrated that OligoG inhibited biofilm formation and disrupted established biofilms, in addition to reducing by up to 512-fold the MIC's of a number of antibiotics including azithromycin, oxytetracycline and ciprofloxacin. OligoG was subsequently shown to disrupt mucin networks in CF sputum, increasing the porosity of the matrix.<sup>148</sup> The interaction of OligoG with mucoid networks were investigated using FTIR spectroscopy, AFM and rheological studies. The oligosaccharide was found to modify the rheological properties of CF sputum, decreasing its viscosity

and elasticity. These changes in properties could make it easier for drugs to cross the mucoid barrier, improving the treatment of lung infections, in addition to facilitating better mucociliary clearance. Further work demonstrated that OligoG could also facilitate a dose dependent reduction in *P. aeruginosa* biofilm volume and thickness, and enabling significant reductions in live cell density (Fig. 8).<sup>149</sup> The mechanism for biofilm disruption by OligoG is proposed to arise from interactions between OligoG and components of the EPS matrix. In confocal microscopy studies,<sup>149</sup> fluorescently-labelled OligoG was present throughout the biofilm, suggesting its effective diffusion within the network. Lectin staining experiments demonstrated that treatment with OligoG led to a reduction in the polysaccharide content of the biofilm, a key structural component. These observations suggest that OligoG may disrupt interactions between negatively charged exopolysaccharides and extracellular DNA with divalent cations such as  $\text{Ca}^{2+}$ , which play a key role in maintaining the structural integrity of the biofilm.<sup>150</sup> Pleasingly, a Phase 1 clinical trial demonstrated that inhalation of OligoG was tolerated well, with no toxicity or adverse effects observed.<sup>151</sup> A Phase 2b study is currently underway.<sup>152</sup>

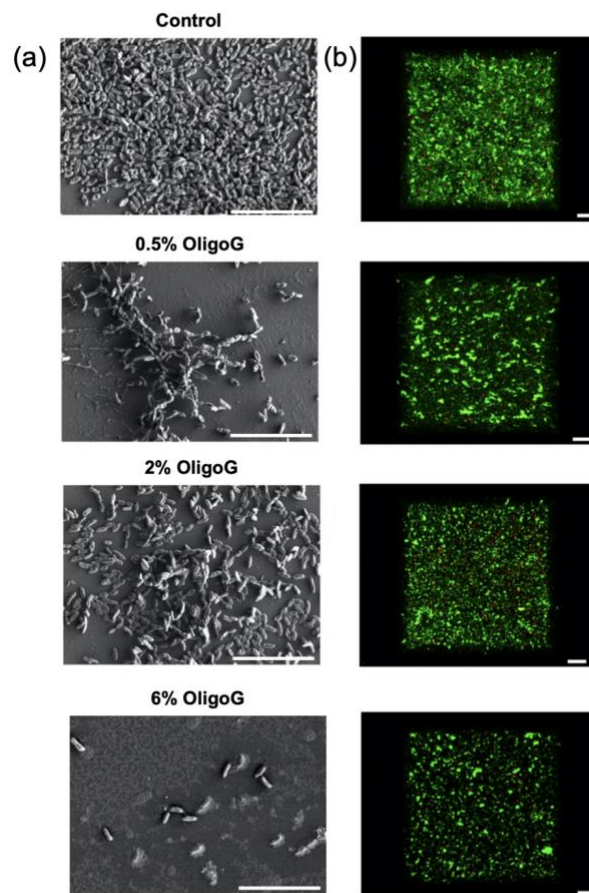


**Fig 8** OligoG inhibition of *P. aeruginosa* biofilm formation,<sup>149</sup> (a) visualized by SEM ( scale bar 10  $\mu\text{m}$ ) and (b) confocal laser scanning microscopy with live/dead staining ( scale bar 20  $\mu\text{m}$ ). Reproduced with permission from reference 149.

In some cases, carbohydrate-binding proteins associated with a bacteria of interest can be targeted to enable more specific action. Biofilm formation in *P. aeruginosa*, for example, is partially enabled through the action of a galactosyl-binding lectin, LecA, and a fucosyl-binding lectin, LecB.<sup>153</sup> Multivalent dendrimers displaying galactose units have been demonstrated to recognise LecA with  $K_d$ 's in the nanomolar range,<sup>154</sup> and inhibit biofilm formation in *in vitro* experiments, with MIC's as low as 10  $\mu\text{M}$  observed. Interestingly, expanding the dendrimer architecture from the second to the third generation, i.e. increasing the number of galactose units displayed from 4 to 8, did not lead to enhancement in inhibition, and further expansion of the dendrimer structure resulted in loss of activity. Detailed crystallography and modelling studies suggested a complex mode of binding, with dendrimers bridging

binding sites on adjacent lectins, an orientation which may not be easily accessible within the architecture of the biofilm. Previously, tetravalent fucose-decorated dendrimers were shown to display similar biofilm inhibition and dispersion properties through interaction with LecB.<sup>155</sup> Heteroglycodendrimers displaying both carbohydrate motifs were subsequently prepared on the same peptide scaffold,<sup>156</sup> with the aim of disrupting the action of both lectins simultaneously. While levels of biofilm inhibition were comparable to those observed with fucosyl- or galactosyl-dendrimers, impressive synergistic effects were observed when glycodendrimers were employed with antimicrobial peptides or tobramycin, an antibiotic commonly used to treat *P. aeruginosa* infections in CF patients, enabling biofilm inhibition and dispersal at sub-inhibitory concentrations of either compound.

Multivalent glycoconjugates based on a calix[4]arene scaffold have been explored by Vidal, Imberty and coworkers as inhibitors of *P. aeruginosa* lectins. Attachment of carbohydrate units to the scaffold via CuAAC affords access to glycoclusters of designed molecular architecture and valency, enabling detailed investigation of the effects of these features. Tetravalent glycoclusters displaying galactosyl motifs were shown to bind to LecA with submicromolar  $K_d$ , as demonstrated by ITC.<sup>157</sup> These glycoconjugates were also shown to inhibit the adhesion of LecA to galactosylated surfaces in surface plasmon resonance (SPR) studies. A later study<sup>158</sup> investigated the binding mode of the glycoclusters to LecA using AFM, revealing that glycoclusters induced aggregative self-assembly to yield monodimensional filaments (Fig. 9). In subsequent work,<sup>159</sup> the calix[4]arene scaffold was modified with either galactose or fucose units. Interactions with complementary lectins, LecA or LecB, were studied by isothermal titration calorimetry (ITC), revealing affinities in the submicromolar to nanomolar range. Tetravalent glycoclusters were demonstrated to interact with PAO1 surface lectins via aggregation assays and were shown to significantly reduce biofilm formation without influencing bacterial growth. The glycoclusters were additionally shown to confer protection against bacteria-induced lung injury in a mouse pulmonary infection model. The affinity of tetravalent galactoclusters based on a mannose scaffold towards LecA was investigated using a range of techniques including enzyme-linked lectin assays (ELLA), ITC and SPR, with  $K_d$  values as low as 157 nM observed.<sup>160</sup> The presence of an aromatic aglycon unit was found to improve the affinity of the glycoclusters for LecA, in line with previous studies.<sup>161-163</sup> The glycoclusters were found to disrupt the formation of *P. aeruginosa* biofilms, with 40% inhibition observed at 10  $\mu$ M concentration. Single cell force spectroscopy, an AFM technique that quantifies interactions between binding partners immobilised on surfaces, was used to probe the effects of these galactoclusters on the adhesion of *P. aeruginosa* to epithelial cells.<sup>164</sup> A human bronchial epithelial cell was attached to the cantilever, and interactions with a *P. aeruginosa* monolayer were investigated by quantifying the detachment force as the cell is withdrawn from the bacterial surface. The addition of glycoclusters to the *P. aeruginosa* monolayer disrupted interactions between cells and bacteria, with the detachment force decreasing by 21%. These studies demonstrate that high-affinity ligands for lectins can disrupt cell-cell interactions, exerting effective anti-adhesive functionality within complex biological environments.

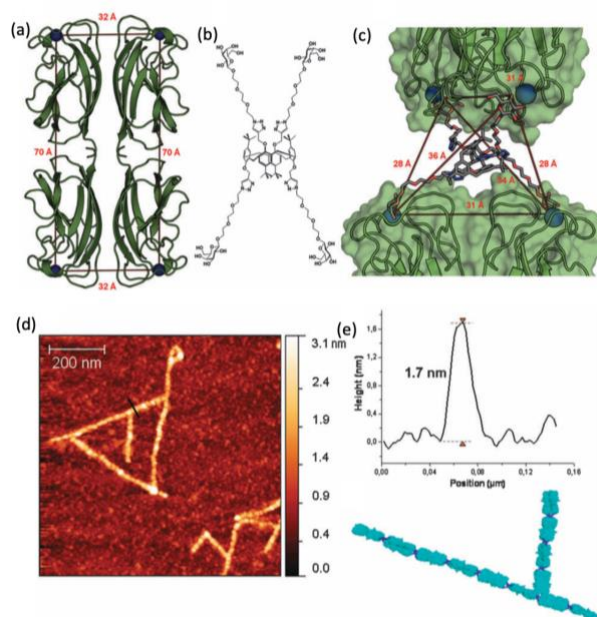


**Fig 9** (a) 3D structure of LecA (1OKO.pdb), with calcium ions in binding sites shown in blue. (b) Calix[4]arene glycocluster. (c) Molecular model of LecA and glycocluster.<sup>157</sup> (d) AFM imaging of filaments formed by LecA and glycocluster on a mica surface, with height profile. (e) Molecular model of 12 lectin tetramers connected by glycoclusters. Reproduced from ref. 158 with permission from The Royal Society of Chemistry.

#### 4. Glycomacromolecular drug delivery systems for antiviral drugs

Viral pathogens, by their nature, present far fewer targets for the development of drugs. Many diseases caused by viruses have been eradicated or can be effectively suppressed through vaccination strategies, such as smallpox, polio and measles, but the development of effective vaccines for other viruses, notably HIV, has thus far proven elusive. Combined with the threat of the emergence of novel viral pathogens, as exemplified by the global impact of the SARS-CoV-2 pandemic (2019-),<sup>165</sup> there is an urgent need to develop effective methods to combat viral disease, with drug delivery systems potentially playing a key role in improving therapeutic outcomes. Key stages in the viral lifecycle include attachment to and entry into the host cell, and release of viral progeny from infected cells. These processes can often be mediated by carbohydrate recognition, and multivalent glycoconjugates have attracted attention as inhibitors, and as candidates for the delivery of vaccines.<sup>9</sup> Here, we will highlight some notable examples of glycomacromolecular systems which present opportunities for the effective delivery of existing antivirals, or in the development of new drugs to treat viral disease, focussing on key pathogens which present global impact.

##### 4.1 Human Immunodeficiency Virus (HIV)

HIV has a substantial global impact, estimated to have accounted for 39 million deaths since its emergence, and more than 36 million people estimated to be living with the disease.<sup>166</sup> HIV damages the immune system, leading to the development of opportunistic infections which can prove fatal. Susceptible cells are infected with the virus through binding of the viral envelope glycoprotein gp120 to a cell surface CD4 receptor, which triggers a series of conformational changes which culminate in membrane fusion and cellular entry of the virus.<sup>167</sup> Within the cytoplasm, the viral RNA genome is reverse-transcribed.<sup>168</sup> HIV is currently managed with a combination of reverse transcriptase inhibitors, commonly based on nucleotide analogues, and protease inhibitors. The intracellular nature of the infection renders treatment complex, with some tissues acting as viral reservoirs, preventing the complete elimination of the virus.<sup>169</sup>

Some progress has been made in the development of drug delivery systems to improve the transport of antiretroviral drugs,<sup>170</sup> with some systems employing polysaccharides as structural components. Azidothymidine triphosphate (AZT-TP) and chitosan were self-assembled via ionotropic gelation,<sup>171</sup> forming nanogels that could deliver AZT-TP, or the natural nucleotide ATP to macrophages, a key target for HIV treatment (Fig. 10). Radiolabelling studies indicated a twofold improvement in AZT-TP uptake compared to the free molecule. In a subsequent study,<sup>172</sup> the incorporation of Fe<sup>3+</sup> ions within the nanogel matrix led to enhanced nanoparticle stability and further improvements in cellular uptake. Chitosan-based nanogels<sup>173</sup> loaded with another antiretroviral drug, saquinavir, were demonstrated to inhibit viral proliferation in T-cells. Another chitosan-based transport system<sup>174</sup> was shown to deliver an AZT prodrug to the cerebrospinal fluid, which can act as a viral reservoir, via nasal administration in a rat model. In another study by Penadés and coworkers,<sup>175</sup> glucose-capped nanoparticles were surface-modified via partial ligand exchange to incorporate aliphatic ester prodrugs of abacavir and lamivudine. Drug-loaded glyconanoparticles displayed similar levels of viral inhibition in cellular assays to free drugs, with IC<sub>50</sub> values of 1-8 μM observed.

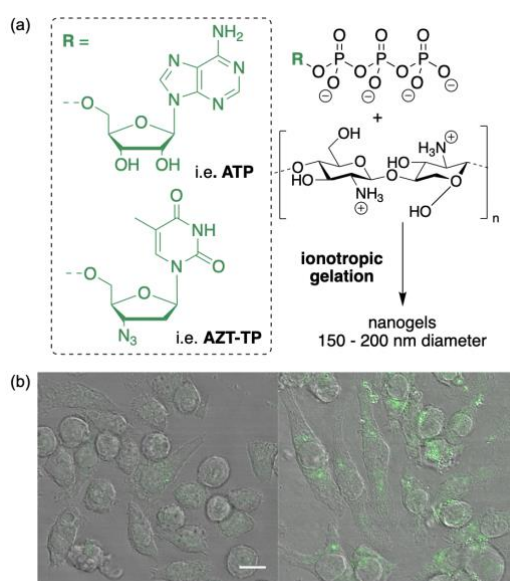


**Fig. 10** (a) Preparation of nanogels loaded with ATP or AZT-TP.<sup>171</sup> (b) Intracellular distribution of fluorescent ATP in J774 cells upon exposure to ATP (left) or ATP-loaded nanogel, imaged using confocal laser microscopy (scale bar = 20 μm). Reprinted (adapted) from *Biomacromolecules*, 2013, **14**, 737-742. Copyright 2013 American Chemical Society.

Another key therapeutic target for HIV is the disruption of the interaction between gp120 and the C-type lectin DC-SIGN (dendritic cell-specific intercellular adhesion molecule grabbing integrin),<sup>176</sup> a mannose-binding receptor expressed on dendritic cells which enables their infection. Infected dendritic cells can *trans*-infect T-cells, enabling replication of the virus. DC-SIGN is a particularly attractive target as it is also implicated in a number of other viral infections, including Ebola, Hepatitis C and Dengue fever.<sup>176</sup> A wide range of multivalent glycoconjugates and glycomimetics based on dendritic scaffolds,<sup>177-180</sup> fullerenes and nanotubes,<sup>181-183</sup> or nanoparticles<sup>184-186</sup> have been explored as DC-SIGN inhibitors, with many displaying impressive inhibitory potencies, presenting opportunities for the development of multi-action systems. In elegant work by Becer and coworkers,<sup>187</sup> for example, β-cyclodextrin based glyoclusters were demonstrated to bind to DC-SIGN with IC<sub>50</sub> values as low as 30 nM. The cyclodextrin cavity could be loaded with saquinavir mesylate, demonstrating promise as a dual-action therapeutic.

#### 4.2 Influenza

Influenza presents significant challenge to global public health efforts, with seasonal epidemics estimated to be responsible for 650,000 deaths per year,<sup>188</sup> and occasional pandemics which can have catastrophic impacts. The H1N1 'Spanish' influenza of 1918, for example, is thought to have infected around one third of the global population, with an estimated death toll of 50-100 million.<sup>189, 190</sup> Annual

vaccination programmes are costly and rely heavily on the accurate prediction of circulating strains, required because of the large antigenic variation within influenza viruses.<sup>191</sup>

Influenza infection is initiated by the binding of a surface glycoprotein, hemagglutinin, to sialic acid residues displayed by epithelial cells of the upper respiratory tract.<sup>192</sup> This recognition process enables entry of the virus into cells via endocytosis, allowing for replication. The release of newly produced virions to infect other cells is also mediated by carbohydrate recognition. Newly-assembled viral particles are attached to the surface of the host cell, and released through the action of a second glycoprotein, neuraminidase, which cleaves sialic acid residues from cell surface receptors.<sup>193</sup> Some currently used drugs e.g Tamiflu (oseltamivir), Relenza (zanamivir), successfully target this key step in the reproductive cycle, but given that future influenza pandemics are highly likely<sup>194</sup> and some strains exhibit resistance,<sup>195, 196</sup> there is a pressing need for the development of new therapies.

Multivalent effects have been explored to increase the inhibitory potency of neuraminidase inhibitors, with promising results.<sup>197</sup> Attachment of multiple copies of zanamivir to a poly(L-glutamine) scaffold,<sup>198</sup> for example, was shown not only to inhibit neuraminidase activity, and therefore the release of newly synthesised virions from infected cells, but also to inhibit the early stages of infection by interfering with intracellular trafficking of endocytosed viruses and virus-endosome fusion. These synergistic effects led to the polyvalent drug displaying a 1,000-10,000-fold improved potency compared to zanamivir, and importantly, the conjugated drug was shown to be effective against zanamivir and oseltamivir resistant strains.<sup>199</sup> The influenza hemagglutinin is another key therapeutic target. A number of multivalent inhibitors have been designed on macromolecular scaffolds including polymers,<sup>200-203</sup> nanoparticles,<sup>204, 205</sup> dendrimers,<sup>206</sup> and virus-like particles,<sup>207, 208</sup> exploiting cluster glycoside effects to enable improvements in potency. In some cases, these glycomacromolecules present promising new drug candidates, in addition to presenting the opportunity to develop multi-function drug delivery systems that could inhibit key therapeutic viral targets, and co-administer other therapeutics to infected tissue.

The glycomacromolecules found in biological systems can provide inspiration for future directions in drug development and delivery. Within the innate immune system, mucin glycoproteins play a key role in preventing adhesion of viral particles to cells. These heavily glycosylated proteins display decoy cell surface recognition motifs, and intercept bacterial and viral pathogens for mucociliary clearance.<sup>209</sup> Bertozzi and coworkers<sup>210</sup> have prepared a 'model glycocalyx' containing glycopeptide based mucin analogues anchored within a lipid membrane. The synthetic mucin mimics were found to frustrate the binding of influenza with underlying glycolipid receptors and slow the kinetics of membrane fusion, providing mechanistic insights into the innate immune response and highlighting opportunities for the development of multivalent glycoconjugates as therapeutics. Polyglycerol sialosides<sup>211</sup> were used to construct nanogels of varying degrees of conformational flexibility which were shown to bind to the surface of a H3N2 influenza strains by TEM and TIRF microscopy. The most flexible nanogels demonstrated impressive inhibitory potency in cell infection assays, with an apparent IC<sub>50</sub> value of 2.3 pM observed, demonstrating the potential of multivalent glycoconjugates in the development of prophylactics for influenza infection. Godula and coworkers<sup>212</sup> used a lipid-bearing RAFT agent to produce sialylated polymers which could insert themselves within the H1N1 viral envelope to produce a mucin-like layer which could be visualised by TEM. While glycopolymer-coated virions were able to infect MDCK cells through action of surface neuraminidases on the sialylated polymers, when glycopolymers were used in combination with oseltamivir the H1N1 virus displayed up to 80% decreased ability to infect cells (Fig. 11). The system was also cleverly adapted to function as a novel screening platform for inhibitors of influenza infection, which better mimics the environment of the upper respiratory tract, revealing previously overlooked compounds that provided similar levels of inhibition to potent neuraminidase inhibitors such as oseltamivir.

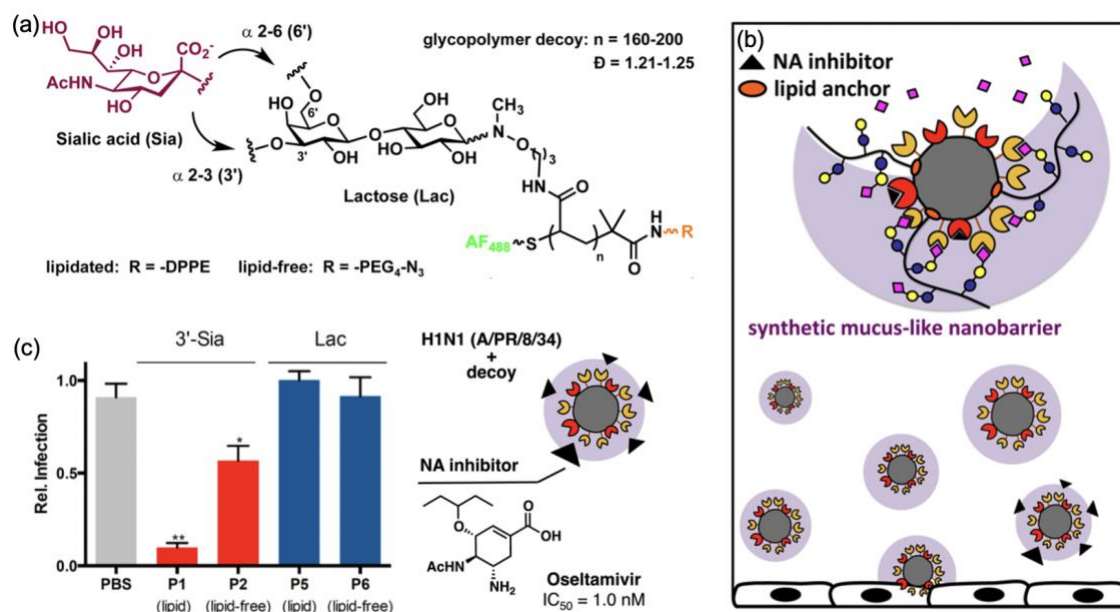


**Fig. 11** (a) Synthetic glycopolymers which mimic the architecture of mucin glycoproteins can insert into the H1N1 viral envelope using a phospholipid tail.<sup>212</sup> (b) Used in combination with neuraminidase inhibitors, mucin-like glycopolymers form a mucus-like barrier around virions, preventing infection. (c) Relative infection rate determined as the ratio of viral activity of modified virions 24 h after inoculation in the presence or absence of oseltamivir. Reprinted (adapted) from *ACS Cent. Sci.*, 2016, **2**, 710-714. Copyright 2016 American Chemical Society.

Similarly inspired by the anti-adhesive action of mucin glycoproteins, Olsen and coworkers<sup>213</sup> synthesised brush polymers displaying peripheral 6-sialyllactose units, via ring-opening metathesis polymerisation (ROMP)<sup>214</sup> of glycosylated norbornenes. ROMP, a living polymerisation technique, enables precise control over the dimensions and ligand density of the resultant polymer brushes,<sup>215, 216</sup> allowing for the investigation of the effects of these structural features during the process of inhibitor design. A densely sialylated brush glycopolymer with backbone length approximately 100 nm was found to be most effective, with an inhibition constant ( $K_i$ ) of 0.24  $\mu$ M observed in an agglutination assay. This brush glycopolymer was also shown to be more effective than a bovine mucin in preventing infection of mammalian cells by influenza. In subsequent work<sup>203</sup> by the same group, mucin-like architectures were constructed by the recombinant expression of homopropargylglycine enriched peptides and subsequent attachment of mannosyl-, lactosyl- or sialosyl- azides. These glycoconjugates displayed similar inhibitory potencies to those observed for brush glycopolymers, and present a more biocompatible scaffold for development of new therapeutics and glycosylated drug delivery systems.

## 5. Outlook

The benefits of using carbohydrates in macromolecular drug delivery systems are clear. They can be used with great effect as structural components to construct stable, biocompatible macromolecular architectures which present pathways for metabolism or biodegradation. Additionally, the carbohydrate recognition processes which impact the onset or progression of disease can be harnessed to facilitate specific targeting of drugs to particular cell types, or pathogens. Many of the glycomacromolecular systems highlighted in this review have demonstrated therapeutic potential in their own right, presenting exciting opportunities for the development drug delivery systems with multiple, distinct modes of action.

Challenges remain, however, before glycomacromolecular drug delivery systems can be employed to their full potential. The polysaccharides used in the construction of drug delivery systems are derived from natural sources, and consequently display varying degrees of structural heterogeneity. The effects of structural parameters such as molecular weight, extent of branching and dispersity on the performance of the resultant delivery system have not often been explored. Further investigation of

these parameters could improve the construction by design of drug delivery systems, enabling robust, reproducible performance.

Another key issue is that of specificity. Most glycomacromolecular drug delivery systems designed to date have employed relatively simple carbohydrate species, predominantly monosaccharides, or readily available disaccharides such as lactose. Effective avidities are realised through the cluster glycoside effect, but the challenge of achieving specific recognition in the complex biological arena remains. Many lectins will recognise multiple monosaccharides with similar affinities,<sup>217</sup> which could be expected to lead to off-target effects *in vivo*. Exploring the use of more complex carbohydrate structures which better reflect the complexity of glycans found in nature, facilitated by advances in synthetic methodology such as automated glycan assembly<sup>143</sup> and advances in chemoenzymatic methods,<sup>142</sup> could open up new exciting possibilities for the development of next generation drug delivery systems.

## Acknowledgement

The authors would like to thank the Durham University Biophysical Sciences Institute for the award of a Summer Research Bursary to W.S-W.

## References

1. O. C. Farokhzad and R. Langer, *ACS Nano*, 2009, **3**, 16-20.
2. M. J. Webber and R. Langer, *Chem. Soc. Rev.*, 2017, **46**, 6600-6620.
3. S. Pottanam Chali and B. J. Ravoo, *Angew. Chem. Int. Ed.*, 2020, **59**, 2962-2972.
4. Z. Li, C. Di, S. Li, X. Yang and G. Nie, *Acc. Chem. Res.*, 2019, **52**, 2703-2712.
5. F. Seidi, R. Jenjob and D. Crespy, *Chem. Rev.*, 2018, **118**, 3965-4036.
6. A. Imberty and A. Varrot, *Curr. Opin. Struct. Biol.*, 2008, **18**, 567-576.
7. J. Grove and M. Marsh, *J. Cell Biol.*, 2011, **195**, 1071-1082.
8. J. Pizarro-Cerdá and P. Cossart, *Cell*, 2006, **124**, 715-727.
9. A. Bernardi, J. Jimenez-Barbero, A. Casnati, C. De Castro, T. Darbre, F. Fieschi, J. Finne, H. Funken, K.-E. Jaeger, M. Lahmann, T. K. Lindhorst, M. Marradi, P. Messner, A. Molinaro, P. V. Murphy, C. Nativi, S. Oscarson, S. Penades, F. Peri, R. J. Pieters, O. Renaudet, J.-L. Reymond, B. Richichi, J. Rojo, F. Sansone, C. Schaffer, W. B. Turnbull, T. Velasco-Torrijos, S. Vidal, S. Vincent, T. Wennekes, H. Zuilhof and A. Imberty, *Chem. Soc. Rev.*, 2013, **42**, 4709-4727.
10. A. Imberty, Y. M. Chabre and R. Roy, *Chem. Eur. J.*, 2008, **14**, 7490-7499.
11. A. Varki, R. D. Cummings, M. Aebi, N. H. Packer, P. H. Seeberger, J. D. Esko, P. Stanley, G. Hart, A. Darvill, T. Kinoshita, J. J. Prestegard, R. L. Schnaar, H. H. Freeze, J. D. Marth, C. R. Bertozzi, M. E. Etzler, M. Frank, J. F. Vliegenthart, T. Lütteke, S. Perez, E. Bolton, P. Rudd, J. Paulson, M. Kanehisa, P. Toukach, K. F. Aoki-Kinoshita, A. Dell, H. Narimatsu, W. York, N. Taniguchi and S. Kornfeld, *Glycobiology*, 2015, **25**, 1323-1324.
12. World Health Organisation Cancer Factsheet, <https://www.who.int/news-room/factsheets/detail/cancer>, (accessed 20/08/2020).
13. K. Strebhardt and A. Ullrich, *Nat. Rev. Cancer*, 2008, **8**, 473-480.
14. A. Beck, L. Goetsch, C. Dumontet and N. Corvaia, *Nat. Rev. Drug. Discov.*, 2017, **16**, 315-337.
15. N. J. Yang and M. J. Hinner, *Methods Mol. Biol.*, 2015, **1266**, 29-53.
16. J. Fang, H. Nakamura and H. Maeda, *Adv. Drug Deliv. Rev.*, 2011, **63**, 136-151.
17. A. Gabizon, R. Catane, B. Uziely, B. Kaufman, T. Safra, R. Cohen, F. Martin, A. Huang and Y. Barenholz, *Cancer Res.*, 1994, **54**, 987-992.
18. T. M. Allen and A. Chonn, *FEBS Lett.*, 1987, **223**, 42-46.
19. K. Babiuch, A. Dag, J. Zhao, H. Lu and M. H. Stenzel, *Biomacromolecules*, 2015, **16**, 1948-1957.
20. F. Suriano, R. Pratt, J. P. K. Tan, N. Wiradharma, A. Nelson, Y.-Y. Yang, P. Dubois and J. L. Hedrick, *Biomaterials*, 2010, **31**, 2637-2645.
21. B. Jana, S. Mohapatra, P. Mondal, S. Barman, K. Pradhan, A. Saha and S. Ghosh, *ACS Appl. Mater. Interfaces*, 2016, **8**, 13793-13803.
22. R. V. Murthy, H. Bavireddi, M. Gade and R. Kikkeri, *ChemMedChem*, 2015, **10**, 792-796.
23. D. Pati, S. Das, N. G. Patil, N. Parekh, D. H. Anjum, V. Dhaware, A. V. Ambade and S. Sen Gupta, *Biomacromolecules*, 2016, **17**, 466-475.
24. P. S. Pramod, R. Shah and M. Jayakannan, *Nanoscale*, 2015, **7**, 6636-6652.

25. Y. Chang, C. Hou, J. Ren, X. Xin, Y. Pei, Y. Lu, S. Cao and Z. Pei, *Chem. Commun.*, 2016, **52**, 9578-9581.
26. Y. Barenholz, *J. Control. Release*, 2012, **160**, 117-134.
27. R.-C. Qian, J. Lv, H.-W. Li and Y.-T. Long, *ChemMedChem*, 2017, **12**, 1823-1827.
28. Q. A. Besford, M. Wojnilowicz, T. Suma, N. Bertleff-Zieschang, F. Caruso and F. Cavaliere, *ACS Appl. Mater. Interfaces*, 2017, **9**, 16869-16879.
29. S. Sungsuwan, Z. Yin and X. Huang, *ACS Appl. Mater. Interfaces*, 2015, **7**, 17535-17544.
30. M. Gary-Bobo, Y. Mir, C. Rouxel, D. Brevet, I. Basile, M. Maynadier, O. Vaillant, O. Mongin, M. Blanchard-Desce, A. Morère, M. Garcia, J.-O. Durand and L. Raehm, *Angew. Chem. Int. Ed.*, 2011, **50**, 11425-11429.
31. X. Wu, Y. J. Tan, H. T. Toh, L. H. Nguyen, S. H. Kho, S. Y. Chew, H. S. Yoon and X.-W. Liu, *Chem. Sci.*, 2017, **8**, 3980-3988.
32. X. Liu, B. Liu, S. Gao, Z. Wang, Y. Tian, M. Wu, S. Jiang and Z. Niu, *J. Mater. Chem. B*, 2017, **5**, 2078-2085.
33. T. Amann, U. Maegdefrau, A. Hartmann, A. Agaimy, J. Marienhagen, T. S. Weiss, O. Stoeltzing, C. Warnecke, J. Schölmerich, P. J. Oefner, M. Kreutz, A. K. Bosserhoff and C. Hellerbrand, *Am. J. Pathol.*, 2009, **174**, 1544-1552.
34. D. Deng, C. Xu, P. Sun, J. Wu, C. Yan, M. Hu and N. Yan, *Nature*, 2014, **510**, 121-125.
35. Y. Li, W. Hong, H. Zhang, T. T. Zhang, Z. Chen, S. Yuan, P. Peng, M. Xiao and L. Xu, *J. Control. Release*, 2020, **317**, 232-245.
36. P. Ma, J. Chen, X. Bi, Z. Li, X. Gao, H. Li, H. Zhu, Y. Huang, J. Qi and Y. Zhang, *ACS Appl. Mater. Interfaces*, 2018, **10**, 12351-12363.
37. X. Pei, F. Luo, J. Zhang, W. Chen, C. Jiang and J. Liu, *Sci. Rep.*, 2017, **7**, 975.
38. K. Shao, N. Ding, S. Huang, S. Ren, Y. Zhang, Y. Kuang, Y. Guo, H. Ma, S. An, Y. Li and C. Jiang, *ACS Nano*, 2014, **8**, 1191-1203.
39. S. Cecioni, A. Imberty and S. Vidal, *Chem. Rev.*, 2015, **115**, 525-561.
40. A. Varki, *Essentials of Glycobiology*, Cold Spring Harbor Press, New York, 2nd edn., 2009.
41. I. Camby, M. Le Mercier, F. Lefranc and R. Kiss, *Glycobiology*, 2006, **16**, 137R-157R.
42. M. Spiess, *Biochemistry*, 1990, **29**, 10009-10018.
43. S. Cao, Z. Pei, Y. Xu and Y. Pei, *Chem. Mater.*, 2016, **28**, 4501-4506.
44. X.-L. Hu, Y. Zang, J. Li, G.-R. Chen, T. D. James, X.-P. He and H. Tian, *Chem. Sci.*, 2016, **7**, 4004-4008.
45. H.-H. Han, C.-Z. Wang, Y. Zang, J. Li, T. D. James and X.-P. He, *Chem. Commun.*, 2017, **53**, 9793-9796.
46. Y. Chang, Y. Lv, P. Wei, P. Zhang, L. Pu, X. Chen, K. Yang, X. Li, Y. Lu, C. Hou, Y. Pei, W. Zeng and Z. Pei, *Adv. Funct. Mater.*, 2017, **27**, 1703083.
47. X. Xia, Z. Zhou, C. DeSantis, J. J. Rossi and D. Bong, *ACS Chem. Biol.*, 2019, **14**, 1310-1318.
48. D. Wienke, G. C. Davies, D. A. Johnson, J. Sturge, M. B. K. Lambros, K. Savage, S. E. Elsheikh, A. R. Green, I. O. Ellis, D. Robertson, J. S. Reis-Filho and C. M. Isacke, *Cancer Res.*, 2007, **67**, 10230-10240.
49. D. H. Dube and C. R. Bertozzi, *Nat. Rev. Drug. Discov.*, 2005, **4**, 477-488.
50. H. Baumann, E. Nudelman, K. Watanabe and S.-i. Hakomori, *Cancer Res.*, 1979, **39**, 2637-2643.
51. D. J. Becker and J. B. Lowe, *Glycobiology*, 2003, **13**, 41R-53R.
52. M. Yoshida, R. Takimoto, K. Murase, Y. Sato, M. Hirakawa, F. Tamura, T. Sato, S. Iyama, T. Osuga, K. Miyanishi, K. Takada, T. Hayashi, M. Kobune and J. Kato, *PLOS ONE*, 2012, **7**, e39545.
53. T. Osuga, R. Takimoto, M. Ono, M. Hirakawa, M. Yoshida, Y. Okagawa, N. Uemura, Y. Arihara, Y. Sato, F. Tamura, T. Sato, S. Iyama, K. Miyanishi, K. Takada, T. Hayashi, M. Kobune and J. Kato, *J. Natl Cancer Inst.*, 2016, **108**.
54. M. E. Davis and M. E. Brewster, *Nat. Rev. Drug. Discov.*, 2004, **3**, 1023-1035.
55. Z. Ye, Q. Zhang, S. Wang, P. Bharate, S. Varela-Aramburu, M. Lu, P. H. Seeberger and J. Yin, *Chem. Eur. J.*, 2016, **22**, 15216-15221.
56. C. J. Day, E. N. Tran, E. A. Semchenko, G. Tram, L. E. Hartley-Tassell, P. S. K. Ng, R. M. King, R. Ulanovsky, S. McAtamney, M. A. Apicella, J. Tiralongo, R. Morona, V. Korolik and M. P. Jennings, *Proc. Natl. Acad. Sci.*, 2015, **112**, E7266-E7275.
57. D. Maiti, X. Tong, X. Mou and K. Yang, *Front Pharmacol.*, 2019, **9**, 01401.
58. A. R. Maity, A. Chakraborty, A. Mondal and N. R. Jana, *Nanoscale*, 2014, **6**, 2752-2758.
59. M. Assali, J.-J. Cid, M. Pernía-Leal, M. Muñoz-Bravo, I. Fernández, R. E. Wellinger and N. Khair, *ACS Nano*, 2013, **7**, 2145-2153.

60. S. Eiben, C. Koch, K. Altintoprak, A. Southan, G. Tovar, S. Laschat, I. M. Weiss and C. Wege, *Adv. Drug Deliv. Rev.*, 2019, **145**, 96-118.
61. A. Klug, *Phil. Trans. R. Soc. Lond. B*, 1999, **354**, 531-535.
62. K. Birsoy, R. Possemato, F. K. Lorbeer, E. C. Bayraktar, P. Thiru, B. Yucel, T. Wang, W. W. Chen, C. B. Clish and D. M. Sabatini, *Nature*, 2014, **508**, 108-112.
63. P. Yuan, K. Ito, R. Perez-Lorenzo, C. Del Guzzo, J. H. Lee, C.-H. Shen, M. W. Bosenberg, M. McMahon, L. C. Cantley and B. Zheng, *Proc. Natl Acad. Sci. U S A*, 2013, **110**, 18226.
64. J. Zhuang, M. R. Gordon, J. Ventura, L. Li and S. Thayumanavan, *Chem. Soc. Rev.*, 2013, **42**, 7421-7435.
65. J. Hu, G. Zhang and S. Liu, *Chem. Soc. Rev.*, 2012, **41**, 5933-5949.
66. C. Justus, L. Dong and L. Yang, *Front. Physiol.*, 2013, **4**.
67. H. J. Forman, H. Zhang and A. Rinna, *Mol. Aspects Med.*, 2009, **30**, 1-12.
68. X.-L. Hu, N. Kwon, K.-C. Yan, A. C. Sedgwick, G.-R. Chen, X.-P. He, T. D. James and J. Yoon, *Adv. Funct. Mater.*, 2020, **30**, 1907906.
69. M. Lan, S. Zhao, W. Liu, C.-S. Lee, W. Zhang and P. Wang, *Adv. Healthcare Mat.*, 2019, **8**, 1900132.
70. Y. Shen, A. J. Shuhendler, D. Ye, J.-J. Xu and H.-Y. Chen, *Chem. Soc. Rev.*, 2016, **45**, 6725-6741.
71. G. Bianchini, J. M. Balko, I. A. Mayer, M. E. Sanders and L. Gianni, *Nat. Rev. Clin. Oncol.*, 2016, **13**, 674-690.
72. D. Brevet, M. Gary-Bobo, L. Raehm, S. Richeter, O. Hocine, K. Amro, B. Loock, P. Couleaud, C. Frochot, A. Morère, P. Maillard, M. Garcia and J.-O. Durand, *Chem. Commun.*, 2009, 1475-1477.
73. Q. Zhang, Y. Cai, Q.-Y. Li, L.-N. Hao, Z. Ma, X.-J. Wang and J. Yin, *Chem. Eur. J.*, 2017, **23**, 14307-14315.
74. X.-L. Hu, Q. Cai, J. Gao, R. A. Field, G.-R. Chen, N. Jia, Y. Zang, J. Li and X.-P. He, *ACS Appl. Mater. Interfaces*, 2019, **11**, 22181-22187.
75. K. A. Whitehead, R. Langer and D. G. Anderson, *Nat. Rev. Drug Discov.*, 2009, **8**, 129-138.
76. Y. Dong, D. J. Siegwart and D. G. Anderson, *Adv. Drug Deliv. Rev.*, 2019, **144**, 133-147.
77. X. Zhao, X. Li, Y. Zhao, Y. Cheng, Y. Yang, Z. Fang, Y. Xie, Y. Liu, Y. Chen, Y. Ouyang and W. Yuan, *Front. Pharmacol.*, 2017, **8**, 00510.
78. P. Xu, G. Bajaj, T. Shugg, W. G. Van Alstine and Y. Yeo, *Biomacromolecules*, 2010, **11**, 2352-2358.
79. C.-C. Lee, Y. Liu and T. M. Reineke, *Bioconj. Chem.*, 2008, **19**, 428-440.
80. Y. Liu, L. Wenning, M. Lynch and T. M. Reineke, *J. Am. Chem. Soc.*, 2004, **126**, 7422-7423.
81. Y. Liu and T. M. Reineke, *J. Am. Chem. Soc.*, 2005, **127**, 3004-3015.
82. Y. Liu and T. M. Reineke, *Bioconj. Chem.*, 2007, **18**, 19-30.
83. Y. Liu and T. M. Reineke, *Biomacromolecules*, 2010, **11**, 316-325.
84. L. Yin, M. C. Dalsin, A. Sizovs, T. M. Reineke and M. A. Hillmyer, *Macromolecules*, 2012, **45**, 4322-4332.
85. C. Van Bruggen, J. K. Hexum, Z. Tan, R. J. Dalal and T. M. Reineke, *Acc. Chem. Res.*, 2019, **52**, 1347-1358.
86. M. E. Davis, *Mol. Pharm.*, 2009, **6**, 659-668.
87. H. Gonzalez, S. J. Hwang and M. E. Davis, *Bioconj. Chem.*, 1999, **10**, 1068-1074.
88. T. M. Reineke and M. E. Davis, *Bioconj. Chem.*, 2003, **14**, 247-254.
89. T. M. Reineke and M. E. Davis, *Bioconj. Chem.*, 2003, **14**, 255-261.
90. S. R. Popielarski, S. Mishra and M. E. Davis, *Bioconj. Chem.*, 2003, **14**, 672-678.
91. M. E. Davis, S. H. Pun, N. C. Bellocq, T. M. Reineke, S. R. Popielarski, S. Mishra and J. D. Heidel, *Curr. Med. Chem.*, 2004, **11**, 179-197.
92. N. C. Bellocq, M. E. Davis, Heidrun Engler, Gregory S. Jensen, A. Liu, T. Machemer, D. C. Maneval, E. Quijano, S. H. Pun, T. Schlupe, Shufen and Wen., *Mol. Ther.*, 2003, **7**, S290.
93. N. C. Bellocq, S. H. Pun, G. S. Jensen and M. E. Davis, *Bioconj. Chem.*, 2003, **14**, 1122-1132.
94. M. E. Davis, J. E. Zuckerman, C. H. J. Choi, D. Seligson, A. Tolcher, C. A. Alabi, Y. Yen, J. D. Heidel and A. Ribas, *Nature*, 2010, **464**, 1067-1070.
95. S. J. Lee, M. S. Huh, S. Y. Lee, S. Min, S. Lee, H. Koo, J.-U. Chu, K. E. Lee, H. Jeon, Y. Choi, K. Choi, Y. Byun, S. Y. Jeong, K. Park, K. Kim and I. C. Kwon, *Angew. Chem. Int. Ed.*, 2012, **51**, 7203-7207.
96. A. E. Smith, A. Sizovs, G. Grandinetti, L. Xue and T. M. Reineke, *Biomacromolecules*, 2011, **12**, 3015-3022.
97. J. Sun, R. Sheng, T. Luo, Z. Wang, H. Li and A. Cao, *J. Mater. Chem. B*, 2016, **4**, 4696-4706.

98. Z. P. Tolstyka, H. Phillips, M. Cortez, Y. Wu, N. Ingle, J. B. Bell, P. B. Hackett and T. M. Reineke, *Acs Biomater. Sci. Eng.*, 2016, **2**, 43-55.
99. S. Perrier, *Macromolecules*, 2017, **50**, 7433-7447.
100. J. De Neve, J. J. Haven, L. Maes and T. Junkers, *Polym. Chem.*, 2018, **9**, 4692-4705.
101. A. Anastasaki, V. Nikolaou and D. M. Haddleton, *Polym. Chem.*, 2016, **7**, 1002-1026.
102. S. Shanmugam and K. Matyjaszewski, in *Reversible Deactivation Radical Polymerization: Mechanisms and Synthetic Methodologies*, American Chemical Society, 2018, vol. 1284, ch. 1, pp. 1-39.
103. S. Quan, P. Kumar and R. Narain, *ACS Biomater. Sci. Eng.*, 2016, **2**, 853-859.
104. Y.-Y. Peng, D. Diaz-Dussan, P. Kumar and R. Narain, *Biomacromolecules*, 2018, **19**, 4052-4058.
105. Y. Chen, D. Diaz-Dussan, Y.-Y. Peng and R. Narain, *Biomacromolecules*, 2019, **20**, 2068-2074.
106. R. J. Mancini, J. Lee and H. D. Maynard, *J. Am. Chem. Soc.*, 2012, **134**, 8474-8479.
107. A. Sizovs, L. Xue, Z. P. Tolstyka, N. P. Ingle, Y. Wu, M. Cortez and T. M. Reineke, *J. Am. Chem. Soc.*, 2013, **135**, 15417-15424.
108. R. Smith and J. Coast, *BMJ*, 2013, **346**.
109. H. H. Tuson and D. B. Weibel, *Soft Matter*, 2013, **9**, 4368-4380.
110. S. Sattin and A. Bernardi, *Trends Biotechnol.*, 2016, **34**, 483-495.
111. J. J. Lundquist and E. J. Toone, *Chem. Rev.*, 2002, **102**, 555-578.
112. A. M. Eissa, A. Abdulkarim, G. J. Sharples and N. R. Cameron, *Biomacromolecules*, 2016, **17**, 2672-2679.
113. M.-H. Xiong, Y.-J. Li, Y. Bao, X.-Z. Yang, B. Hu and J. Wang, *Adv. Mater.*, 2012, **24**, 6175-6180.
114. F. Liu, L. Bai, H. Zhang, H. Song, L. Hu, Y. Wu and X. Ba, *ACS Appl. Mater. Interfaces*, 2017, **9**, 31626-31633.
115. L. B. Capeletti, J. F. A. de Oliveira, L. M. D. Loiola, F. E. Galdino, D. E. D. Santos, T. A. Soares, R. D. Freitas and M. B. Cardoso, *Adv. Funct. Mater.*, 2019, **29**, 11.
116. H.-C. Flemming, J. Wingender, U. Szewzyk, P. Steinberg, S. A. Rice and S. Kjelleberg, *Nat. Rev. Microbiol.*, 2016, **14**, 563-575.
117. T. Bjarnsholt, *APMIS*, 2013, **121**, 1-58.
118. C. Winstanley, S. O'Brien and M. A. Brockhurst, *Trends Microbiol.*, 2016, **24**, 327-337.
119. L. K. Jennings, K. M. Storek, H. E. Ledvina, C. Coulon, L. S. Marmont, I. Sadovskaya, P. R. Secor, B. S. Tseng, M. Scian, A. Filloux, D. J. Wozniak, P. L. Howell and M. R. Parsek, *Proc. Natl Acad. Sci. U S A*, 2015, **112**, 11353.
120. H. Koo, R. N. Allan, R. P. Howlin, P. Stoodley and L. Hall-Stoodley, *Nat. Rev. Microbiol.*, 2017, **15**, 740-755.
121. L. R. Martinez, M. R. Mihu, M. Tar, R. J. B. Cordero, G. Han, A. J. Friedman, J. M. Friedman and J. D. Nosanchuk, *J. Infect. Dis.*, 2010, **201**, 1436-1440.
122. S. H. Bang, I. C. Hwang, Y. M. Yu, H. R. Kwon, D. H. Kim and H. J. Park, *J. Microencapsulation*, 2011, **28**, 595-604.
123. A. Machul, D. Mikołajczyk, A. Regiel-Futyra, P. B. Heczko, M. Strus, M. Arruebo, G. Stochel and A. Kyzioł, *J. Biomater. Appl.*, 2015, **30**, 269-278.
124. E. I. Rabea, M. E. T. Badawy, C. V. Stevens, G. Smagghe and W. Steurbaut, *Biomacromolecules*, 2003, **4**, 1457-1465.
125. S. E. Birk, J. A. J. Haagensen, H. K. Johansen, S. Molin, L. H. Nielsen and A. Boisen, *Adv. Healthcare Mater.*, 2020, **9**, 1901779.
126. Y. Tan, S. Ma, M. Leonhard, D. Moser, G. M. Haselmann, J. Wang, D. Eder and B. Schneider-Stickler, *Carbohydr. Polym.*, 2018, **200**, 35-42.
127. Y. Qiu, D. Xu, G. Sui, D. Wang, M. Wu, L. Han, H. Mu and J. Duan, *Int. J. Biol. Macromol.*, 2020, **156**, 640-647.
128. K. K. Patel, M. Tripathi, N. Pandey, A. K. Agrawal, S. Gade, M. M. Anjum, R. Tilak and S. Singh, *Int. J. Pharm.*, 2019, **563**, 30-42.
129. J. Cao, Y. Zhao, Y. Liu, S. Tian, C. Zheng, C. Liu, Y. Zhai, Y. An, H. J. Busscher, L. Shi and Y. Liu, *ACS Macro Lett.*, 2019, **8**, 651-657.
130. D. P. Arora, S. Hossain, Y. Xu and E. M. Boon, *Biochemistry*, 2015, **54**, 3717-3728.
131. A. W. Carpenter and M. H. Schoenfish, *Chem. Soc. Rev.*, 2012, **41**, 3742-3752.
132. D. A. Riccio and M. H. Schoenfish, *Chem. Soc. Rev.*, 2012, **41**, 3731-3741.
133. Z. Sadrearhami, J. Yeow, T.-K. Nguyen, K. K. K. Ho, N. Kumar and C. Boyer, *Chem. Commun.*, 2017, **53**, 12894-12897.

134. T.-K. Nguyen, R. Selvanayagam, K. K. K. Ho, R. Chen, S. K. Kutty, S. A. Rice, N. Kumar, N. Barraud, H. T. T. Duong and C. Boyer, *Chem. Sci.*, 2016, **7**, 1016-1027.
135. R. Namivandi-Zangeneh, Z. Sadrearhami, A. Bagheri, M. Sauvage-Nguyen, K. K. K. Ho, N. Kumar, E. H. H. Wong and C. Boyer, *ACS Macro Letters*, 2018, **7**, 592-597.
136. Y. Lu, D. L. Slomberg, A. Shah and M. H. Schoenfish, *Biomacromolecules*, 2013, **14**, 3589-3598.
137. Y. Lu, D. L. Slomberg and M. H. Schoenfish, *Biomaterials*, 2014, **35**, 1716-1724.
138. K. P. Reighard, C. Ehre, Z. L. Rushton, M. J. R. Ahonen, D. B. Hill and M. H. Schoenfish, *ACS Biomater. Sci. Eng.*, 2017, **3**, 1017-1026.
139. J. P. Quiñones, H. Peniche and C. Peniche, *Polymers*, 2018, **10**, 235.
140. R. Li, X. Yuan, J. Wei, X. Zhang, G. Cheng, Z. A. Wang and Y. Du, *Mar. Drugs*, 2019, **17**.
141. M. L. Sobel, G. A. McKay and K. Poole, *Antimicrob. Agents Chemother.*, 2003, **47**, 3202.
142. P. J. Smith, M. E. Ortiz-Soto, C. Roth, W. J. Barnes, J. Seibel, B. R. Urbanowicz and F. Pfrengele, *ACS Sustainable Chem. Eng.*, 2020, **8**, 11853-11871.
143. M. Guberman and P. H. Seeberger, *J. Am. Chem. Soc.*, 2019, **141**, 5581-5592.
144. M. F. Moradali and B. H. A. Rehm, *Nat. Rev. Microbiol.*, 2020, **18**, 195-210.
145. K. Y. Lee and D. J. Mooney, *Prog. Polym. Sci.*, 2012, **37**, 106-126.
146. S. Khan, A. Tøndervik, H. Sletta, G. Klinkenberg, C. Emanuel, E. Onsøyen, R. Myrvold, R. A. Howe, T. R. Walsh, K. E. Hill and D. W. Thomas, *Antimicrob. Agents Chemother.*, 2012, **56**, 5134-5141.
147. L. C. Powell, M. F. Pritchard, C. Emanuel, E. Onsøyen, P. D. Rye, C. J. Wright, K. E. Hill and D. W. Thomas, *Am. J. Respir. Cell Mol. Biol.*, 2014, **50**, 483-492.
148. M. F. Pritchard, L. C. Powell, G. E. Menzies, P. D. Lewis, K. Hawkins, C. Wright, I. Doull, T. R. Walsh, E. Onsoyen, A. Dessen, R. Myrvold, P. D. Rye, A. H. Myrset, H. N. Stevens, L. A. Hodges, G. MacGregor, J. B. Neilly, K. E. Hill and D. W. Thomas, *Mol. Pharm.*, 2016, **13**, 863-872.
149. L. C. Powell, M. F. Pritchard, E. L. Ferguson, K. A. Powell, S. U. Patel, P. D. Rye, S.-M. Sakellakou, N. J. Burma, C. D. Brilliant, J. M. Copping, G. E. Menzies, P. D. Lewis, K. E. Hill and D. W. Thomas, *npj Biofilms Microbiomes*, 2018, **4**, 13.
150. T. Das, S. Sehar, L. Koop, Y. K. Wong, S. Ahmed, K. S. Siddiqui and M. Manefield, *PLOS ONE*, 2014, **9**, e91935.
151. Safety and Efficacy of Inhaled OligoG CF-5/20 for the Treatment Cystic Fibrosis, <https://ClinicalTrials.gov/show/NCT00970346>).
152. A Phase 2b Randomised, Placebo Controlled Study of OligoG in Patients With Cystic Fibrosis, <https://ClinicalTrials.gov/show/NCT03822455>).
153. C. Chemani, A. Imberty, S. de Bentzmann, M. Pierre, M. Wimmerová, B. P. Guery and K. Faure, *Infect. Immun.*, 2009, **77**, 2065-2075.
154. M. Bergmann, G. Michaud, R. Visini, X. Jin, E. Gillon, A. Stocker, A. Imberty, T. Darbre and J. L. Reymond, *Org. Biomol. Chem.*, 2016, **14**, 138-148.
155. E. M. V. Johansson, S. A. Cruz, E. Kolomiets, L. Buts, R. U. Kadam, M. Cacciarini, K.-M. Bartels, S. P. Diggle, M. Cámara, P. Williams, R. Loris, C. Nativi, F. Rosenau, K.-E. Jaeger, T. Darbre and J.-L. Reymond, *Chem. Biol.*, 2008, **15**, 1249-1257.
156. G. Michaud, R. Visini, M. Bergmann, G. Salerno, R. Bosco, E. Gillon, B. Richichi, C. Nativi, A. Imberty, A. Stocker, T. Darbre and J.-L. Reymond, *Chem. Sci.*, 2016, **7**, 166-182.
157. S. Cecioni, R. Lalor, B. Blanchard, J.-P. Praly, A. Imberty, S. E. Matthews and S. Vidal, *Chem. Eur. J.*, 2009, **15**, 13232-13240.
158. D. Sicard, S. Cecioni, M. Iazykov, Y. Chevolut, S. E. Matthews, J.-P. Praly, E. Souteyrand, A. Imberty, S. Vidal and M. Phaner-Goutorbe, *Chem. Commun.*, 2011, **47**, 9483-9485.
159. A. M. Boukerb, A. Rousset, N. Galanos, J.-B. Méar, M. Thépaut, T. Grandjean, E. Gillon, S. Cecioni, C. Abderrahmen, K. Faure, D. Redelberger, E. Kipnis, R. Dessein, S. Havet, B. Darblade, S. E. Matthews, S. de Bentzmann, B. Guéry, B. Cournoyer, A. Imberty and S. Vidal, *J. Med. Chem.*, 2014, **57**, 10275-10289.
160. C. Ligeour, O. Vidal, L. Dupin, F. Casoni, E. Gillon, A. Meyer, S. Vidal, G. Vergoten, J.-M. Lacroix, E. Souteyrand, A. Imberty, J.-J. Vasseur, Y. Chevolut and F. Morvan, *Org. Biomol. Chem.*, 2015, **13**, 8433-8444.
161. F. Casoni, L. Dupin, G. Vergoten, A. Meyer, C. Ligeour, T. Géhin, O. Vidal, E. Souteyrand, J.-J. Vasseur, Y. Chevolut and F. Morvan, *Org. Biomol. Chem.*, 2014, **12**, 9166-9179.
162. J. Rodrigue, G. Ganne, B. Blanchard, C. Saucier, D. Giguère, T. C. Shiao, A. Varrot, A. Imberty and R. Roy, *Org. Biomol. Chem.*, 2013, **11**, 6906-6918.

163. B. Gerland, A. Goudot, C. Ligeour, G. Pourceau, A. Meyer, S. Vidal, T. Gehin, O. Vidal, E. Souteyrand, J.-J. Vasseur, Y. Chevolut and F. Morvan, *Bioconj. Chem.*, 2014, **25**, 379-392.
164. F. Zuttion, C. Ligeour, O. Vidal, M. Wälte, F. Morvan, S. Vidal, J.-J. Vasseur, Y. Chevolut, M. Phaner-Goutorbe and H. Schillers, *Nanoscale*, 2018, **10**, 12771-12778.
165. G. Li and E. De Clercq, *Nat. Rev. Drug Discov.*, 2020, **19**, 149-150.
166. A. Pandey and A. P. Galvani, *Lancet HIV*, 2019, **6**, e809-e811.
167. P. J. Klasse, *Cell. Microbiol.*, 2012, **14**, 1183-1192.
168. E. J. Arts and D. J. Hazuda, *Cold Spring Harb. Perspect. Med.*, 2012, **2**.
169. C. Katlama, S. G. Deeks, B. Autran, J. Martinez-Picado, J. van Lunzen, C. Rouzioux, M. Miller, S. Vella, J. E. Schmitz, J. Ahlers, D. D. Richman and R. P. Sekaly, *Lancet*, 2013, **381**, 2109-2117.
170. A. Sosnik and R. Augustine, *Adv. Drug Deliv. Rev.*, 2016, **103**, 105-120.
171. G. Giacalone, A. Bochot, E. Fattal and H. Hillaireau, *Biomacromolecules*, 2013, **14**, 737-742.
172. G. Giacalone, H. Hillaireau, P. Capiou, H. Chacun, F. Reynaud and E. Fattal, *J. Control. Release*, 2014, **194**, 211-219.
173. L. N. Ramana, S. Sharma, S. Sethuraman, U. Ranga and U. M. Krishnan, *Biochim. Biophys. Acta*, 2014, **1840**, 476-484.
174. A. Dalpiaz, M. Fogagnolo, L. Ferraro, A. Capuzzo, B. Pavan, G. Rassu, A. Salis, P. Giunchedi and E. Gavini, *Antiviral Res.*, 2015, **123**, 146-157.
175. F. Chiodo, M. Marradi, J. Calvo, E. Yuste and S. Penadés, *Beilstein J. Org. Chem*, 2014, **10**, 1339-1346.
176. Y. van Kooyk and T. B. H. Geijtenbeek, *Nat. Rev. Immunol.*, 2003, **3**, 697-709.
177. L. Medve, S. Achilli, J. Guzman-Caldentey, M. Thépaut, L. Senaldi, A. Le Roy, S. Sattin, C. Ebel, C. Vivès, S. Martin-Santamaria, A. Bernardi and F. Fieschi, *Chem. Eur. J.*, 2019, **25**, 14659-14668.
178. S. Ordanini, N. Varga, V. Porkolab, M. Thépaut, L. Belvisi, A. Bertaglia, A. Palmioli, A. Berzi, D. Trabattoni, M. Clerici, F. Fieschi and A. Bernardi, *Chem. Commun.*, 2015, **51**, 3816-3819.
179. V. Porkolab, E. Chabrol, N. Varga, S. Ordanini, I. Sutkevičiūtė, M. Thépaut, M. J. García-Jiménez, E. Girard, P. M. Nieto, A. Bernardi and F. Fieschi, *ACS Chem. Biol.*, 2018, **13**, 600-608.
180. S. Sattin, A. Daggetti, M. Thépaut, A. Berzi, M. Sánchez-Navarro, G. Tabarani, J. Rojo, F. Fieschi, M. Clerici and A. Bernardi, *ACS Chem. Biol.*, 2010, **5**, 301-312.
181. L. Rodríguez-Pérez, J. Ramos-Soriano, A. Pérez-Sánchez, B. M. Illescas, A. Muñoz, J. Luczkowiak, F. Lasala, J. Rojo, R. Delgado and N. Martín, *J. Am. Chem. Soc.*, 2018, **140**, 9891-9898.
182. A. Muñoz, D. Sigwalt, B. M. Illescas, J. Luczkowiak, L. Rodríguez-Pérez, I. Nierengarten, M. Holler, J.-S. Remy, K. Buffet, S. P. Vincent, J. Rojo, R. Delgado, J.-F. Nierengarten and N. Martín, *Nature Chem.*, 2016, **8**, 50-57.
183. J. Ramos-Soriano, J. J. Reina, B. M. Illescas, N. de la Cruz, L. Rodríguez-Pérez, F. Lasala, J. Rojo, R. Delgado and N. Martín, *J. Am. Chem. Soc.*, 2019, **141**, 15403-15412.
184. O. Martínez-Ávila, K. Hijazi, M. Marradi, C. Clavel, C. Champion, C. Kelly and S. Penadés, *Chem. Eur. J.*, 2009, **15**, 9874-9888.
185. Y. Guo, C. Sakonsinsiri, I. Nehlmeier, M. A. Fascione, H. Zhang, W. Wang, S. Pöhlmann, W. B. Turnbull and D. Zhou, *Angew. Chem. Int. Ed.*, 2016, **55**, 4738-4742.
186. Y. Guo, I. Nehlmeier, E. Poole, C. Sakonsinsiri, N. Hondow, A. Brown, Q. Li, S. Li, J. Whitworth, Z. Li, A. Yu, R. Brydson, W. B. Turnbull, S. Pöhlmann and D. Zhou, *J. Am. Chem. Soc.*, 2017, **139**, 11833-11844.
187. Q. Zhang, L. Su, J. Collins, G. Chen, R. Wallis, D. A. Mitchell, D. M. Haddleton and C. R. Becer, *J. Am. Chem. Soc.*, 2014, **136**, 4325-4332.
188. World Health Organisation: Influenza – estimating burden of disease, <https://www.euro.who.int/en/health-topics/communicable-diseases/influenza/seasonal-influenza/burden-of-influenza>, (accessed 30/09/2020).
189. J. K. Taubenberger and D. M. Morens, *Emerg. Infect. Dis.*, 2006, **12**, 15-22.
190. N. P. Johnson and J. Mueller, *Bull. Hist. Med.*, 2002, **76**, 105-115.
191. B. S. Hamilton, G. R. Whittaker and S. Daniel, *Viruses*, 2012, **4**.
192. J. J. Skehel and D. C. Wiley, *Annu. Rev. Biochem.*, 2000, **69**, 531-569.
193. J. L. McAuley, B. P. Gilbertson, S. Trifkovic, L. E. Brown and J. L. McKimm-Breschkin, *Front. Microbiol.*, 2019, **10**.
194. M. C. Crank, J. R. Mascola and B. S. Graham, *J. Infect. Dis.*, 2019, **219**, S107-S109.

195. N. J. Dharan, L. V. Gubareva, J. J. Meyer, M. Okomo-Adhiambo, R. C. McClinton, S. A. Marshall, K. St. George, S. Epperson, L. Brammer, A. I. Klimov, J. S. Bresee, A. M. Fry and f. t. Oseltamivir-Resistance Working Group, *JAMA*, 2009, **301**, 1034-1041.
196. F. G. Hayden and M. D. de Jong, *J. Infect. Dis.*, 2011, **203**, 6-10.
197. M. Stanley, N. Cattle, J. McCauley, S. R. Martin, A. Rashid, R. A. Field, B. Carbain and H. Streicher, *MedChemComm*, 2012, **3**, 1373-1376.
198. C. M. Lee, A. K. Weight, J. Haldar, L. Wang, A. M. Klibanov and J. Chen, *Proc. Natl Acad. Sci. U S A*, 2012, **109**, 20385.
199. A. K. Weight, J. Haldar, L. Á. de Cienfuegos, L. V. Gubareva, T. M. Tumpey, J. Chen and A. M. Klibanov, *J. Pharm. Sci.*, 2011, **100**, 831-835.
200. M. Nagao, Y. Fujiwara, T. Matsubara, Y. Hoshino, T. Sato and Y. Miura, *Biomacromolecules*, 2017, **18**, 4385-4392.
201. M. Nagao, T. Matsubara, Y. Hoshino, T. Sato and Y. Miura, *Biomacromolecules*, 2019, **20**, 2763-2769.
202. M. Nagao, T. Matsubara, Y. Hoshino, T. Sato and Y. Miura, *Bioconj. Chem.*, 2019, **30**, 1192-1198.
203. B. M. Seifried, W. Qi, Y. J. Yang, D. J. Mai, W. B. Puryear, J. A. Runstadler, G. Chen and B. D. Olsen, *Bioconj. Chem.*, 2020, **31**, 554-566.
204. V. Poonthiyil, P. T. Nagesh, M. Husain, V. B. Golovko and A. J. Fairbanks, *ChemistryOpen*, 2015, **4**, 708-716.
205. M. Ogata, S. Umemura, N. Sugiyama, N. Kuwano, A. Koizumi, T. Sawada, M. Yanase, T. Takaha, J.-i. Kadokawa and T. Usui, *Carbohydr. Polym.*, 2016, **153**, 96-104.
206. S. Bhatia, D. Lauster, M. Bardua, K. Ludwig, S. Angioletti-Uberti, N. Popp, U. Hoffmann, F. Paulus, M. Budt, M. Stadtmüller, T. Wolff, A. Hamann, C. Böttcher, A. Herrmann and R. Haag, *Biomaterials*, 2017, **138**, 22-34.
207. C. Nie, B. Parshad, S. Bhatia, C. Cheng, M. Stadtmüller, A. Oehrl, Y. Kerkhoff, T. Wolff and R. Haag, *Angew. Chem. Int. Ed.*, 2020, **59**, 15532-15536.
208. D. Lauster, S. Klenk, K. Ludwig, S. Nojumi, S. Behren, L. Adam, M. Stadtmüller, S. Saenger, S. Zimmer, K. Hönzke, L. Yao, U. Hoffmann, M. Bardua, A. Hamann, M. Witzenrath, L. E. Sander, T. Wolff, A. C. Hocke, S. Hippenstiel, S. De Carlo, J. Neudecker, K. Osterrieder, N. Budisa, R. R. Netz, C. Böttcher, S. Liese, A. Herrmann and C. P. R. Hackenberger, *Nat. Nanotechnol.*, 2020, **15**, 373-379.
209. M. C. Rose and J. A. Voynow, *Phys. Rev.*, 2006, **86**, 245-278.
210. C. S. Delaveris, E. R. Webster, S. M. Banik, S. G. Boxer and C. R. Bertozzi, *Proc. Natl Acad. Sci. U S A*, 2020, **117**, 12643.
211. S. Bhatia, M. Hilsch, J. L. Cuellar-Camacho, K. Ludwig, C. Nie, B. Parshad, M. Wallert, S. Block, D. Lauster, C. Böttcher, A. Herrmann and R. Haag, *Angew. Chem. Int. Ed.*, 2020, **59**, 12417-12422.
212. M. Cohen, H. P. Senaati, C. J. Fisher, M. L. Huang, P. Gagneux and K. Godula, *ACS Cent. Sci.*, 2016, **2**, 710-714.
213. S. Tang, W. B. Puryear, B. M. Seifried, X. Dong, J. A. Runstadler, K. Ribbeck and B. D. Olsen, *ACS Macro Lett.*, 2016, **5**, 413-418.
214. C. W. Bielawski and R. H. Grubbs, in *Controlled and Living Polymerizations*, eds. A. H. E. Müller and K. Matyjaszewski, 2009, ch. 6.
215. T.-P. Lin, A. B. Chang, H.-Y. Chen, A. L. Liberman-Martin, C. M. Bates, M. J. Voegtle, C. A. Bauer and R. H. Grubbs, *J. Am. Chem. Soc.*, 2017, **139**, 3896-3903.
216. T. Pelras, C. S. Mahon and M. Müllner, *Angew. Chem. Int. Ed.*, 2018, **57**, 6982-6994.
217. S. Tommasone, F. Allabush, Y. K. Tagger, J. Norman, M. Köpf, J. H. R. Tucker and P. M. Mendes, *Chem. Soc. Rev.*, 2019, **48**, 5488-5505.